ILLINOIS CENTER FOR TRANSPORTATION

CIVIL ENGINEERING STUDIES
Illinois Center for Transportation Series No. 21-002
UILU-ENG-2021-2002
ISSN: 0197-9191

Truck-Platoonable Pavement Sections in Illinois' Network

Prepared By
Imad L. Al-Qadi
Egemen Okte
Aravind Ramakrishnan
Qingwen Zhou
Watheq Sayeh
University of Illinois at Urbana-Champaign

Research Report No. FHWA-ICT-21-002

The first of two reports of the findings of

ICT PROJECT R27-203
Truck Platooning on Illinois Flexible Pavements

https://doi.org/10.36501/0197-9191/21-002

Illinois Center for Transportation

February 2021

TECHNICAL REPORT DOCUMENTATION PAGE

1. Report No. FHWA-ICT-21-002	**2. Government Accession No.** N/A	**3. Recipient's Catalog No.** N/A
4. Title and Subtitle Truck-Platoonable Pavement Sections in Illinois' Network		**5. Report Date** February 2021 **6. Performing Organization Code** N/A
7. Authors Imad L. Al-Qadi (https://orcid.org/0000-0002-5824-103X), Egemen Okte, Aravind Ramakrishnan, Qingwen Zhou, Watheq Sayeh		**8. Performing Organization Report No.** ICT-21-002 UILU-2021-2002
9. Performing Organization Name and Address Illinois Center for Transportation Department of Civil and Environmental Engineering University of Illinois at Urbana-Champaign 205 North Mathews Avenue, MC-250 Urbana, IL 61801		**10. Work Unit No.** N/A **11. Contract or Grant No.** R27-203
12. Sponsoring Agency Name and Address Illinois Department of Transportation (SPR) Bureau of Research 126 East Ash Street Springfield, IL 62704		**13. Type of Report and Period Covered** Interim Report 6/1/19–5/31/21 **14. Sponsoring Agency Code**

15. Supplementary Notes
Conducted in cooperation with the U.S. Department of Transportation, Federal Highway Administration.
https://doi.org/10.36501/0197-9191/21-002

16. Abstract
Truck platooning has many benefits over traditional truck mobility. Literature shows that platooning improves safety and reduces fuel consumption between 5% and 15% based on platoon configuration. In Illinois, trucks carry more than 50% of freight tonnage and constitute 25% of the traffic on interstates. Deployment of truck platooning within interstate highways would result in significant fuel savings, but may have a direct impact on flexible pavement performance. The channelization of the platoon and reduced rest time between consecutive loads would accelerate the damage accumulation at the channelized position. Ultimately, this would lead to pavement service life reduction and a subsequent increase in maintenance and rehabilitation costs. Therefore, the main objective of this project is to quantify the effects of platooning on flexible pavements and provide guidelines for the state of Illinois by considering the aforementioned factors. Although the benefits of platooning are quantifiable, not every truck route is platoonable. For efficient platooning, trucks need to travel at a constant high speed for extended distances. The integrity of the platoon should be preserved because interfering vehicles would compromise the platooning benefits and road safety. An introduced high-level approach considers the volume/capacity of a roadway and the expected number of highway exit and entry conflicts. Using these parameters, each roadway section is assigned a level of platoonability, ranging from one to five—with five being the highest. A framework was developed to analyze the Illinois highway network. It was found that 89% of the network highway is platoonable under average capacity conditions.

17. Key Words Truck Platooning, Platoonable Segments, Resting Period, Fuel Consumption	**18. Distribution Statement** No restrictions. This document is available through the National Technical Information Service, Springfield, VA 22161.

19. Security Classif. (of this report) Unclassified	**20. Security Classif. (of this page)** Unclassified	**21. No. of Pages** 44	**22. Price** N/A

Form DOT F 1700.7 (8-72) **Reproduction of completed page authorized**

ACKNOWLEDGMENT, DISCLAIMER, MANUFACTURERS' NAMES

This publication is based on the results of **ICT-R27-203: Truck Platooning on Illinois Pavements**. ICT-R27-203 was conducted in cooperation with the Illinois Center for Transportation; the Illinois Department of Transportation; and the U.S. Department of Transportation, Federal Highway Administration.

Members of the Technical Review Panel (TRP) were the following:

- Brian Hill, TRP Co-chair, Illinois Department of Transportation
- Charles Wienrank, TRP Co-chair, Illinois Department of Transportation
- Dennis Bachman, Federal Highway Administration
- Autumn Bizon, Freight Management Inc.
- Kevin Burke, Illinois Asphalt Pavement Association
- Anabelle Huff, Illinois Department of Transportation
- Joseph Kuhlman, Illinois Department of Transportation
- LaDonna Rowden, Illinois Department of Transportation
- Laura Shanley, Illinois Department of Transportation
- Megan Swanson, Illinois Department of Transportation
- Shawn Wilcockson, Illinois Department of Transportation

TABLE OF CONTENTS

LIST OF FIGURES

LIST OF TABLES

CHAPTER 1: INTRODUCTION

OVERVIEW

The growing truck traffic and freight demand has created two major issues for the trucking industry. The first is the shortage of truck drivers. According to the American Trucking Associations, the current driver shortage is around 60,800 and is expected to increase to 1.1 million over the next decade (Costello and Karickhoff 2019). The second issue is increasing operation cost due to congestion. In 2014, according to the American Trucking Research Institute, congestion caused over $49 billion in additional operation cost in the United States. This added operation cost may raise the price of transported goods (Pierce and Murray 2014). To address these issues, technological developments have been introduced in the trucking industry. One such recent innovation is implementing connected and autonomous vehicle (CAV) technology on trucks.

The introduction of connected and autonomous trucks (CATs) in freight transportation is expected to bring many advantages, including addressing the limitations associated with human drivers and reducing operation costs. For example, currently in the United States, truck drivers are not allowed to work more than 11 hours per day and 60 hours per week. This restriction can be relaxed even with limited level of automation (e.g., level 4) where the presence of a human is required within a truck. Ideally, under the assumption of full automation, the operation time may be extended to as high as 24 hours, which can significantly improve the efficiency of freight transportation and lower the cost. The operation cost reduction is achieved through truck platooning, which is defined as a convoy of trucks traveling at a close distance. The enabling communication technologies embedded in CATs may reduce the safe distance between trucks to 10 ft from 200 ft (the current safe norm in the United States). Reducing congestion and braking/accelerating, as well as improving safety, traffic flow, and fuel efficiency are some reported and expected benefits of platooning.

Platooning is characterized by three parameters: spacing between trucks, trucks' speed, and the lateral position of the trucks. These three parameters affect hot-mix asphalt (HMA) deformation, HMA recovery, and healing as well as the rate of damage. This would result in flexible pavement life reduction and an increase in maintenance and rehabilitation costs (Gungor et al. 2019). However, current pavement design guidelines do not consider the aforementioned factors, and a design based on the existing guidelines might underestimate the effects of truck platooning. Therefore, it is important to optimize the design and improve existing guidelines so that the impact of platooning can be minimized on the pavement and maximized for fuel savings.

OBJECTIVES

As truck platooning is transitioning from a concept to reality, agencies and DOTs should be prepared and well informed about the effects of truck platoons on pavements. Therefore, the main objective of this study is to quantify the effects of CAT platoons on flexible pavements and to develop a recommendation for the state of Illinois' consideration of a tradeoff between CAT platoon fuel consumption and accelerated pavement damage. To meet the main objective, several tasks were established. The tasks will be completed in the following order:

1. Determination of platoonable sections of Illinois truck routes and extraction of their section geometries.

2. Determination of flexible pavement damage as a function of trucks' lateral positions, spacing, and number of trucks in a platoon.

3. Determination of the safe, minimum truck spacing by considering flexible pavement damage and traffic congestion.

4. Determination of the optimum platoon design to minimize fuel consumption and damage.

5. Determination of the impact of platoons on environment and costs, such as the life cycle analysis and life cycle cost analysis, respectively.

In this report, a literature review on platooning and the platoonable sections in Illinois are identified and presented in Chapters 2 and 3, respectively. An additional report will focus on the impact on pavement (Al-Qadi et al. 2021).

CHAPTER 2: CURRENT STATE OF KNOWLEDGE ON PLATOONING

A systematic literature review was conducted to examine existing research that is relevant in addressing the research's objectives. This chapter is divided into five categories, including the following: the impact of platooning on fuel efficiency, platoonable sections, impact of a resting period on pavement performance, wheel wander in the pavement design, and the lateral position of CAT.

IMPACT OF PLATOONING ON FUEL EFFICIENCY

The main advantage of placing trucks at a close distance is reducing the overall aerodynamic drag. Most of the aerodynamic drag, approximately 70% to 90%, is caused by the pressure difference, known as the pressure drag, between the front and rear of a truck, also referred to as the high- and low-pressure zones, respectively (Gaudet 2014). In a platoon, the pressure drag on trailing trucks decreases because the trucks in front block the air and lowers the pressure in the frontal zone. For leading trucks, the aerodynamic drag decreases because the trailing truck compresses the turbulent flow that increases the pressure in the low-pressure zone. Consequently, this reduction in aerodynamic drag leads to decreased fuel consumption and increased fuel efficiency.

Numerous studies have attempted to quantify the reduction in fuel consumption due to platooning. The first field study excluded wind tunnel tests and was conducted in the mid-1990s within the scope of a European Union project called "Chauffeur" (Bonnet et al. 2004). The tested platoon composed of two tandem trucks weighing 14.5 tons (leading truck) and 28 tons (trailing truck), respectively. While the leading truck was driven manually, the trailing truck was operated autonomously using an electronic two-bar system. Two sets of experiments were conducted. In the first set, trucks were operated at 50 mph with an intervehicle distance of 22, 23, 26, 33, 39, 46, and 53 ft. The second set reduced the speed to 37 mph and the intervehicle distances to 16, 20, 26, 33, 39, 46, and 53 ft. For each experiment, the trucks completed a 7.5-mi oval level track. Figure 1 presents the fuel saving results. For the trailing truck, the highest fuel efficiency was observed at an intervehicle distance of 26 ft and 16 ft for 50 mph and 37 mph, respectively.

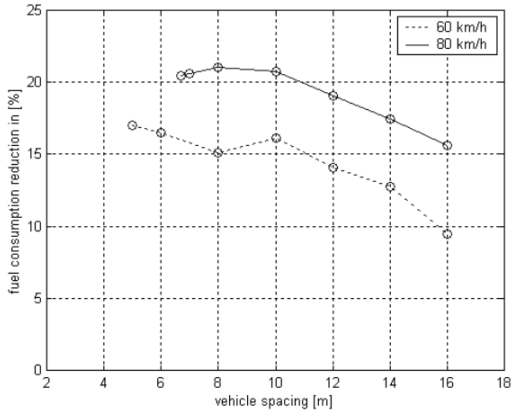

Figure 1. Graph. Percentage reduction in fuel consumption based on test results. (1m = 3.3ft, 1km = 0.62 miles)
Source: Bonnet et al. 2000

In 2004, a platoon consisting of two empty 16-ft-long trucks with varying spacing (i.e., 10, 13, 20, 26, and 33 ft) were tested on an unused road by the California Partners for Advanced Transportation Technology (PATH) program (Browand et al. 2004). The length of the track at the facility was 1.5 mi. The trucks were linked by an electronic control system. Two different speeds were selected: 50 and 56 mph. The results are presented in Figure 2. For leading trucks, the maximum fuel saving achieved was 9% at the smallest intervehicle distance (i.e., 10 ft), which conforms to the previous study (Bonnet et al. 2004). For the trailing truck, optimum spacing was found to be 13 ft, and that led to 12% fuel savings. In that study, the effects of slope and wind on fuel consumption were evaluated as well.

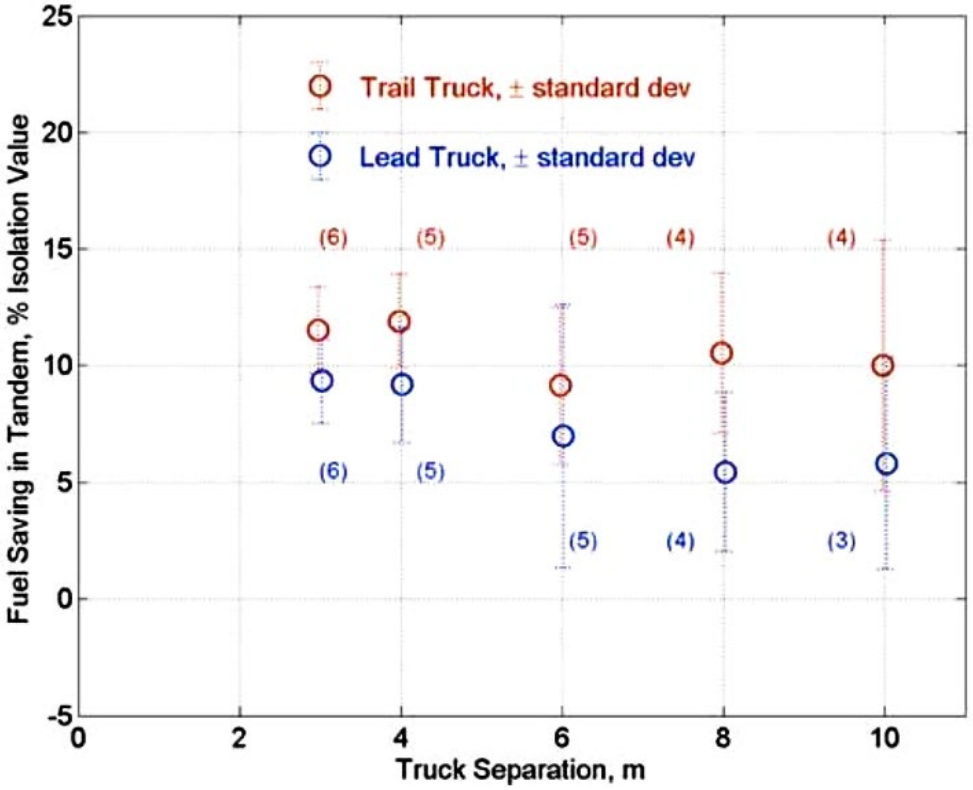

Figure 2. Graph. Fuel saving versus truck separation (1m = 3.3ft).

Source: Browand et al. 2004

In 2011, a platoon, formed by three class-8 tractor-trailer trucks, was tested on an actual highway in Austin, Nebraska, by the PATH program (Lu and Shladover 2014). The study aimed to capture the effects of slopes and curves on fuel efficiency. The trucks were connected using 5.9 GHz Dedicated Short-Range Communications (DSRC) with 100 msec update intervals. The cruising speed was determined at 53 mph. Fuel reductions at this speed with an intervehicle distance of 20 ft were computed as 4.3%, 10%, and 14% for the first, second, and third truck, respectively. The altitude of the test track was 1.1 mi, and the air density was 80% of sea-level air density. The authors noted that the fuel savings would be significantly higher for platoons travelling at regions with lower altitudes. Furthermore, the report indicated that there was an intentional lateral offset between the first and second trucks that decreased fuel efficiency.

In 2008, a project named Energy ITS was launched in Japan, where a platoon of three fully automated heavy trucks and a light truck were tested as shown in Figure 3 (Sadayuki 2014). The trucks were not loaded, and they travelled at a speed of 50 mph. The trucks were linked by 5.8 GHz DSRC, and they were equipped with 76 GHz radar, lidar, and camera sensors for object and lane-mark detections essential for fully autonomous driving. In terms of fuel efficiency, the greatest improvement observed, approximately 24%, occurred in the second truck at 13 ft of spacing (see Figure 4). It is also interesting to note that the results show the third truck's fuel efficiency was unaffected by the intervehicle spacing.

Figure 3. Photo. Truck platoon in Energy ITS project.

Source: Sadayuki 2014

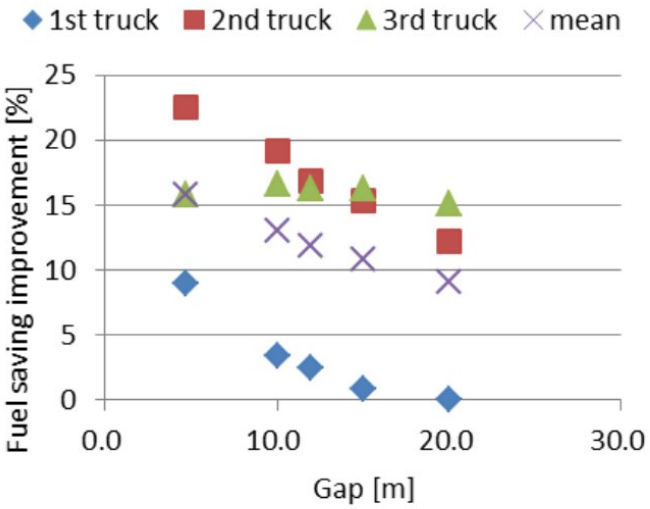

Figure 4. Graph. Fuel savings versus truck spacing (1m = 3.3ft).

Source: Sadayuki 2014

The European Union sponsored the Safe Road Trains for the Environment (SARTRE) project, which studied vehicle platooning under mix-traffic conditions—both autonomous and human-driven vehicles (Chan 2016). The tested platoon was composed of five vehicles, including two heavy trucks

followed by three passenger vehicles. While the first vehicle was driven manually, the following vehicles were equipped with lidar, radar, DSRC, and camera systems to enable fully autonomous driving. The vehicles operated at 56 mph, and the intervehicle distance varied between 13 ft and 82 ft. Reported fuel reduction for the leading truck matches reasonably well with Energy ITS study (see Figure 5). For the second vehicle, the trailing truck, however, had approximately a 10% discrepancy between the two studies. This can be attributed to the fact that the third vehicle in SARTRE was a passenger vehicle as opposed to a heavy truck as seen in the Energy ITS study. Note that the passenger vehicle, right behind the second truck, had much lower fuel reduction compared to the succeeding passenger vehicles. In general, various studies reported that platoons decreased fuel consumption between 5% and 15%, depending on the platoon configuration (Lammert et al. 2014; Deng et al. 2014; Bonnet and Fritz 2000; Tsugawa et al. 2016).

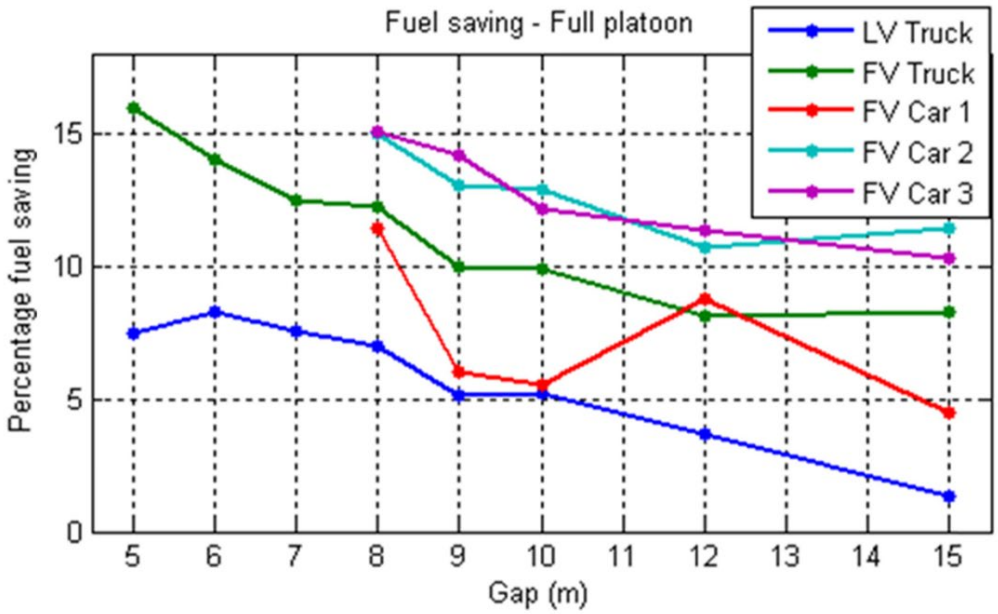

Figure 5. Graph. Fuel saving results of platooning vehicles (1m = 3.3ft).

Source: Chan 2016

PLATOONABLE SECTIONS

Platoonable sections are road sections where truck platooning occurs with minimum to no interruptions due to traffic. The first step for truck platooning implementation is to identify the platoonable road sections. The efficiency of platoons is dependent on the ability to travel at free-flow speed. Therefore, identifying traffic limits for efficient platooning is a challenge (Calvert et al. 2019; Nowakowski et al. 2016). Although safety improvement was indicated as a platooning benefit, real-life data are still lacking (Van Nunen et al. 2017; Carbaugh et al. 1998; Bergenhem et al. 2012).

Although the benefits of platooning could be quantified, not every designated truck route is platoonable. For efficient platooning, trucks need to travel at a constant high speed for an extended distance without any interruptions. Moreover, the integrity of the platoon should be preserved as

interfering vehicles compromise the platooning benefits (Nowakowski et al. 2015). To identify platoonable sections, the National Renewable Energy Lab studied more than three million miles of truck trips. They identified the percentage of miles that trucks were able to travel at 50 mph or greater for more than 15 min, which is the criteria used to identify platooning. Results showed that at the speed thresholds of 50 and 55 mph, respectively, 76.6% and 64.6% of the miles driven were platoonable (Muratori et al. 2017). Although the study suggested an estimate of the platoonable miles, no framework was presented to determine the platoonability of a road section.

Truck platooning would be impacted by vehicle maneuvers near highway exit and entry ramps (Nowakowski et al. 2016; Calvert et al. 2019; Duret et al. 2018). Yet, up to 9% of traffic may be unable to merge in time if the platoon formation does not allow for such maneuver (Wang et al. 2019). Multiple strategies have been suggested to address this issue, including increasing the spacing between trucks near highway entry and exit ramps or allowing trucks to change lanes near the ramps (Van Maarseveen 2017). The latter strategy may jeopardize roadway safety. McAuliffe et al. (2017) reported that increasing vehicle separation from 60 ft to 80 ft at 50 mph decreased fuel consumption savings by approximately 2.5%. Moreover, increasing and decreasing the spacing in a platoon induces extra acceleration and deceleration, which can further decrease cost savings (Deng et al. 2014). Nowakowski et al. (2016) suggests increasing truck spacing may not always be a feasible solution because vehicles may break the platoon by cutting into it. Thus, platoons will be affected by highway entrance and exit ramps. The abovementioned factors were considered in determining the platoonability of a road section.

IMPACT OF RESTING PERIOD ON FLEXIBLE PAVEMENT PERFORMANCE

With the introduction of platooning, the resting time—the period between two consecutive loads—is expected to decrease significantly. This reduction may have detrimental effects on pavements and needs to be studied. The impact of reduced resting time on HMA performance can be grouped into two categories, fatigue and rutting. Resting time on concrete pavement will mainly affect the base erosion. The effect on HMA is discussed herein through the remainder of this report.

Resting Period and Fatigue

It is well reported in the literature that with adequate cracking resistance HMA has a self-healing capability by recovering microcracks when pavement is not loaded (Kim and Little 1989, 1994). Introducing a rest period between two consecutive loads is expected to increase HMA's service life. Self-healing occurs simultaneously with viscoelastic relaxation of HMA, which also affects its fatigue life. Thus, it is important to separate the effects of viscoelastic relaxation from microcrack healing.

In 1989, Kim and Little presented a methodology using Schapery's correspondence principle to isolate the effect of microcrack healing due to resting time. The methodology was evaluated using a cyclic crack-propagation test in which rest periods were introduced randomly. The test occurred in a uniaxial model on an HMA beam with and without a notch. The study presented a healing index based on pseudo-energy density to quantify the impact of the resting period on microcrack healing. The results proved that introducing resting increased HMA's fatigue life because of the recovery of microcracks.

Kim and Little (1994) conducted a follow-up study, where one of the topics covered was demonstrating the existence of the microcrack healing due to resting time in the field. They took to the outer lane of the US 70 highway in Clayton, North Carolina, where traffic was closed for 24 hours. The 1-year-old pavement had 5.5 in of HMA laid over its 11-in-thick aggregate base course. Thermocouples were placed at various depths within the HMA layer to monitor temperature changes during the day. A wave propagation test predicted the modulus at various depths. The test took place right after the lane closure, and it was then repeated hourly for 24 hours. Moduli values were compared at selected temperatures both before and after traffic. Higher moduli were obtained at the end of the 24-hr period, which attributed to the microcrack healing resulted from the resting time.

Hsu and Tseng (1996) used a third-point, flexural fatigue test to quantify the resting period's impact on fatigue performance of HMA mixes. The effects of asphalt binder content and temperature were also studied. The study reported that the number of repetitions to failure increased as the resting time increased. Also, the effect of the resting period on fatigue performance became more significant at lower temperatures and higher asphalt binder contents. The study also conducted theoretical analysis for simulating fatigue damage using linear elastic fracture mechanics and Schapery's (1975) theory of viscoelastic media crack growth, which requires conducting indirect tension and creep tests (Tseng and Lytton 1990). Experimental results were in good agreement with the theoretical simulations.

Lee and Kim (1998) introduced a viscoelastic constitutive model that simulates rate-dependent damage growth and microdamage healing in HMA. The model is an extension of an elastic continuum damage model based on thermodynamics of irreversible processes with an internal state variable. The study developed a mode-independent mechanistic model for fatigue damage prediction, which is applicable for both strain- and stress-controlled tests. A tensile, uniaxial cyclic test was used to obtain the model parameters. For validation purposes, the same test was performed at randomly introduced resting times. A good agreement was observed between the constitutive model and the experimental results. The performance of the model was more accurate for strain-controlled tests compared to that of stress-controlled tests. The authors claimed that complicated strain history from stress-controlled tests might affect the accuracy of the pseudo-strain computation. Another possible reason is the fact that the model parameters were computed from strain-controlled tests and then extrapolated for stress-controlled tests.

Daniel and Kim (2001) also used the third-point flexure fatigue (TFFT) test for studying healing characteristics of HMA mixes under three damage levels—low, medium, and high—and two temperatures—68° and 140°F. The experiments were performed on two different HMA mixes (SHRP AAD-1 and AAM-1). For each mix, three specimens were prepared. The experiments started with conducting a stress-wave test to compute undamaged, elastic moduli for all specimens. Later, TFFT with 3,000 repetitions were conducted on two specimens to induce low-level damage. Later, the healing quantification step was conducted, which entailed computing the moduli of the two specimens using the stress-wave test. Then, the two specimens healed at different temperatures, being exposed to 68°F and 140°F for 4 hours, respectively. Later, both specimens were conditioned at 68°F. As a last step of the healing quantification, damaged moduli were measured using the stress-wave test. After the healing quantification, TFFT with 10,000 repetitions were performed to identify

the medium damage. Then, the healing quantification step was repeated. TFFT was then performed at high damage, entailing 20,000 repetitions, which was followed by the healing quantification step. Finally, TFFT was conducted on all three specimens, two damaged and one undamaged, until they failed. The results from these series of experiments showed that the resting period increased the number of repetitions to failure. Results also indicated the resting period increased elastic modulus and that healing occurred faster at higher temperatures (see Figure 6). Additionally, the healing characteristics significantly vary between HMA mixes.

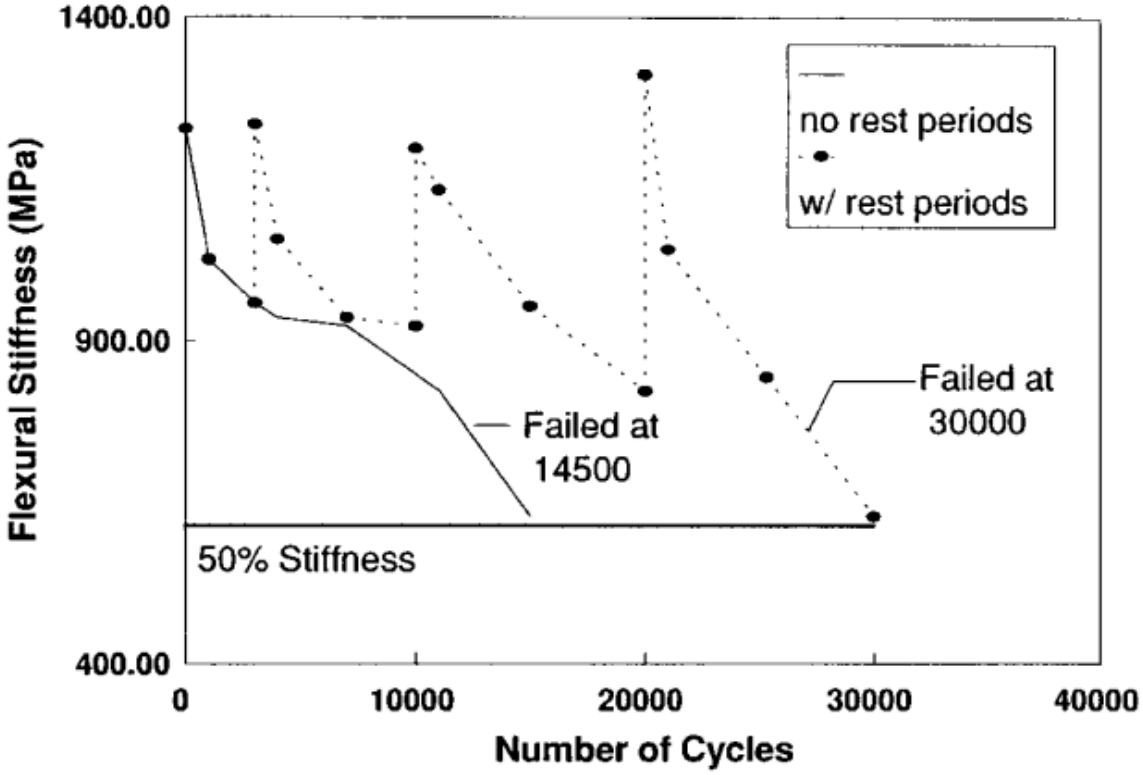

Figure 6. Graph. Flexural stiffness versus number of cycles (1 MPa = 0.145 ksi).

Source: Daniel and Kim 2001

Castro and Sanchez (2006) modified the existing three-point flexure test by applying the load in an intermittent pattern to study the effects of resting time on HMA fatigue. The test was conducted with varying load levels. For lightly loaded specimens, such as long fatigue lives, fatigue life increased by 10 times because of the resting time. This increase was reduced to five times for heavily loaded specimens. This could be related to the extended damage due to macrocracks of heavily loaded specimens, which makes it difficult to heal.

Carpenter and Shen (2006) introduced a specifically designed fatigue-healing test to study HMA fatigue life and self-healing. The test was a modified version of a four-point flexural test with intermittently applied haversine loading. Test results were analyzed based on a previously developed approach called the ratio of dissipated energy change (RDEC). This approach attempts to explain the cause behind damage accumulation given the dissipated energy difference after the loading and

unloading steps. The plateau value—the energy difference at 50% stiffness reduction—is correlated to the number of repetitions to fail. The study conducted a series of experiments using the RDEC approach and concluded that the HMA fatigue life could be increased up to a factor of 10 by introducing a rest period between loadings. Also, the healing might not be observed at high damage levels. The fatigue endurance limit could be studied and computed using RDEC approach, and the polymer-modified HMA mixes exhibit a faster healing rate as compared to HMA mixes with neat binder. A follow-up study conducted by Beranek and Carpenter (2009) introduced a transfer function based on both laboratory and field tests that explicitly takes the resting period as the input and output for the number of repetitions to fail.

$$N_f = 9500.6\,(RP + 1) + 6146.7$$

Figure 7. Equation. The calculation of the number of cycles to fail.

Here N_f is the number of repetitions to fail and RP is the rest period (seconds).

Shan et al. (2010) considered thixotropy to analyze fatigue and healing characteristics of asphalt binders, which they define as "the continuous decrease of viscosity (or material properties generally) with time when a sample, previously at rest, is subjected to flow." The study started with conducting experiments to obtain fatigue and healing characteristics of asphalt binders. Later, the insights from the experimental results were interpreted using thixotropy. The healing test results conformed to that shown in the literature in that the introduction of resting time leads to self-healing. The healing rate changes significantly with respect to the binder content and type. The study demonstrated that thixotropy could be used to understand the long-term behavior of asphalt binders.

Palvadi et al. (2012) utilized the viscoelastic continuum-damage theory to quantify healing in asphalt binder compositions. The results from the theoretical simulations were verified by fatigue experiments with resting periods. They verified the conclusion from previous studies that healing was more significant at lower damage levels and that the introduction of a resting period increased the HMA fatigue life.

Underwood and Zeiada (2014) employed a smeared continuum-damage approach to characterize microdamage healing in HMA. One of the study's objectives was to confirm that the resting period had a profound effect on fatigue response of HMA using modern materials and protocols. The experimental results demonstrated that a rest between loads improved the HMA's fatigue response. Another objective was to determine whether there was a significant difference between the block- and pulse-rest loading applications while assessing HMA healing (see Figure 8). The results exhibited an important difference between the applications as the actual traffic-loading pattern was a combination of those two types. The study suggested the need to capture the realistic loading pattern on HMA fatigue assessment.

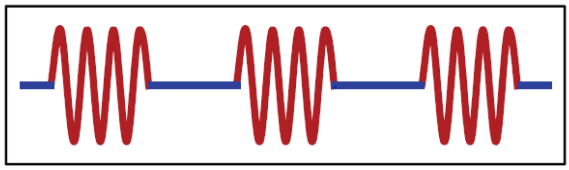

(a) Block rest

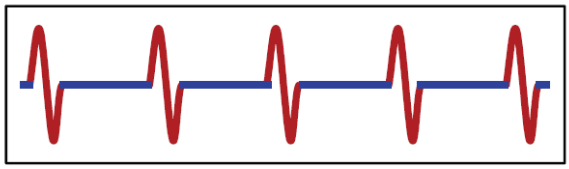

(b) Pulse rest

Figure 8. Photo. Comparison of a block rest versus a pulse rest.

Source: Underwood and Zeiada 2014

Resting Period and Asphalt Concrete Rutting

When HMA is loaded and unloaded, the resultant strain has four components: elastic, viscoelastic, plastic, and viscoplastic. Elastic strain refers to the strain that is immediately recovered when the load is removed. The plastic strain is unrecoverable and immediately occurs when a load is applied. Viscoelastic and viscoplastic strains are time dependent. Viscoelastic strains are recoverable while viscoplastic strains are unrecoverable (Figure 9). The permanent strain, such as normalized rutting, is a summation of the plastic, viscoelastic, and viscoplastic strains. Thus, the permanent strain has two components that are time dependent, and it is affected by both resting times and time of loading.

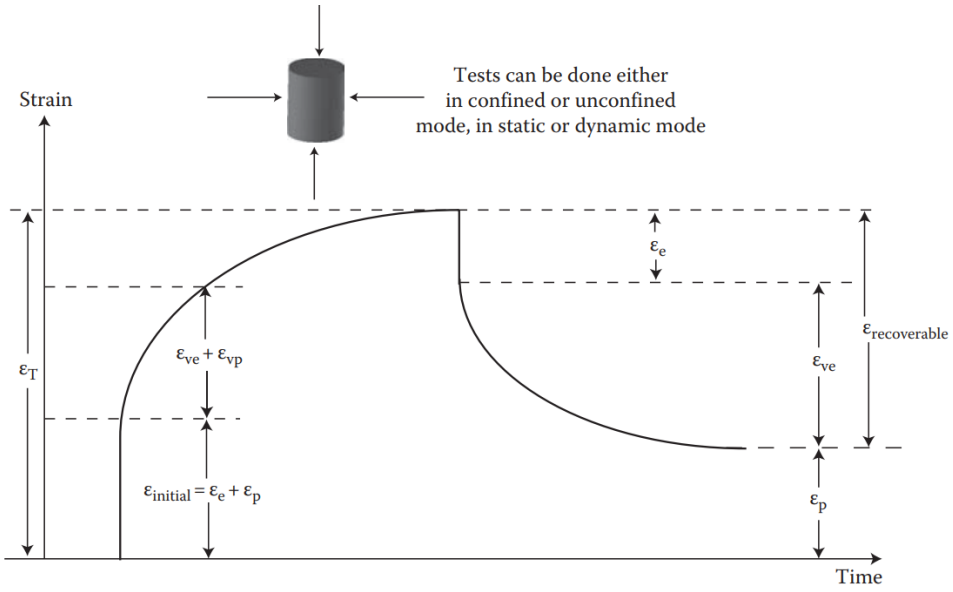

Figure 9. Photo. Components of strain in a creep testing

Source: Mallick and Tahar 2013

Qi and Witczak (1998) conducted a series of unconfined creep loads with varying loading and resting times, stresses, and temperatures. Test results showed that the permanent strain increased as the resting time decreased and the time of loading increased. The study produced a regression model to predict the permanent strain as a function of the loading and resting times, temperatures, and stresses (see Figure 10).

$$\varepsilon_p = \alpha N^b$$

$$\alpha = 3.9682\ x\ 10^{-10}\ t_l^{0.237091} t_r^{-0.096151} T^{2.53870} \sigma^{8.834338}$$

$$b = 0.248371 - 0.0438023\ log(t_l) + 0.0231006\ log(t_r)$$

Figure 10. Equation. Regression equations for permanent deformation.

where epsilon$_p$ is the plastic strain; N is number of repetitions; t_l is time of loading; and t_r is resting time.

In 2012, Darabi et al. (2012) introduced a modified viscoplastic model for predicting permanent deformation of HMA under cyclic-compression loading at high temperatures. The developed model takes viscoplastic softening, such as hardening relaxation, into account while simulating permanent deformation. The authors indicated that the HMA hardened under loading and softened during unloading. When a new cycle starts after unloading, the softened HMA may have higher viscoplastic strain as compared to the end of the previous load cycle. Darabi et al. (2012) conducted a creep-recovery test to validate the developed model. Some of the results showed that viscoplastic strain increased as the rest period expanded.

Nejad et al. (2015) conducted a series of creep-recovery tests under different loading patterns to study the HMA's hardening-relaxation and healing properties. Tests were conducted at 77°F. The loading patterns consisted of four groups: continuous loading with no resting period; intermittent loading, which has a resting period after each load application; pseudo loading, which has a resting period after a series of load applications; and pseudo-continuous loading, which has long rest intervals. For each group, loading and unloading times varied. Each loading-unloading configuration were referred to as a pattern.

Figure 11 and Figure 12 demonstrate intermittent loading and pseudo-continuous loading with short rest intervals for a single pattern, respectively. All patterns were repeated for 120,000 cycles. The results showed that introducing a rest period led to lower permanent deformation within the pavement. In the intermittent loading case, the viscoplastic strain increased with an increasing resting period. This aligns with the previously introduced hardening-relaxation phenomenon of HMA. Hardening relaxation, however, was not observed in the pseudo-continuous loading case. The study experimentally demonstrated a complicated relationship between HMA's resting period and rutting development. It appears that intermittent loading applications may not be enough to model rutting accumulation within HMA; loading patterns should be considered. Similar conclusions were also reported by Underwood and Zeida (2014) for fatigue cracking.

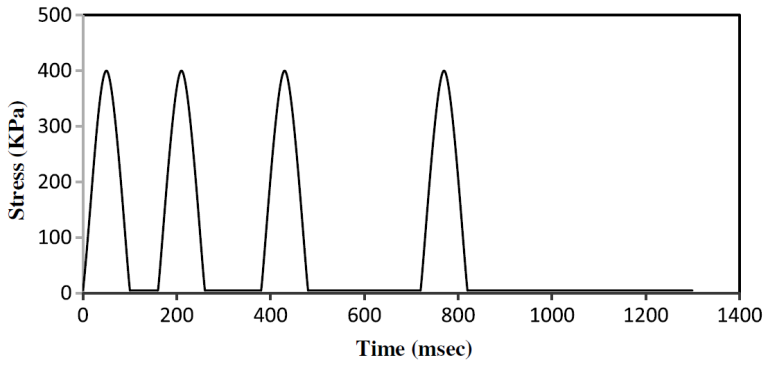

Figure 11. Graph. Pattern A in intermittent loading. The repeating loading blocks are: 100 msec-loading, 60 msec-resting, 100 msec-loading, 120 msec-resting, 100 msec-loading, 240 msec-resting,100 msec-loading, and 480 msec-resting (1 kPa = 0.145 psi).

Source: Nejad et al. 2015

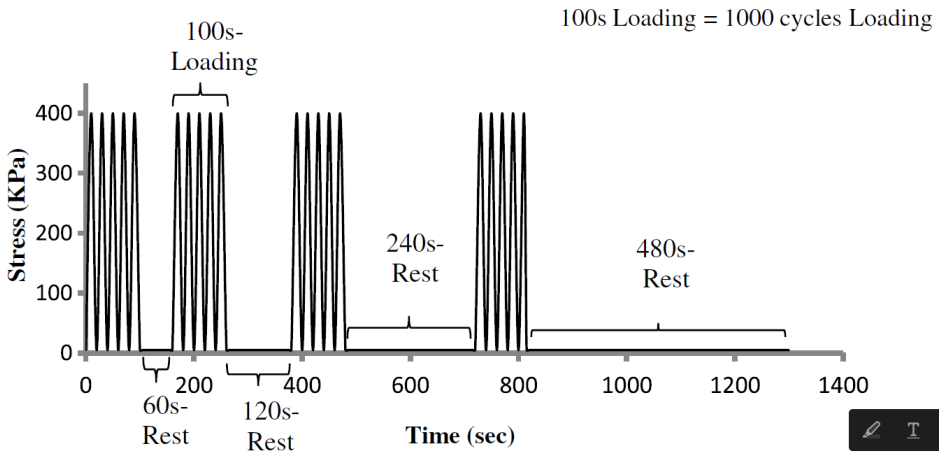

Figure 12. Graph. Pattern B in pseudo-loading with short resting intervals (1 kPa = 0.145 psi).

Source: Nejad et al. 2015

Mansourkhaki et al. (2014) quantified the impact of axle type, including single, tandem, and tridem axels, on HMA's rutting behavior. A series of creep-recovery tests were conducted by changing the pulse duration and resting times under different stress levels. The results showed that the tridem axle is the most damaging axle type. Furthermore, stress levels have a significant effect on the rutting accumulation within HMA.

Motevalizadeh et al. (2018) used repeated loading permanent deformation test to study the impact of the loading and resting times, stress levels, and temperatures on HMA rutting accumulation. Temperature was found to be the most critical variable for HMA permanent deformation behavior. The resting period has a significant impact on rutting accumulation rate, especially at the initial stage.

Furthermore, the study presented a regression model for predicting rutting as a function of temperatures, stress levels, and the loading and resting periods, as shown in Figure 13.

$$\varepsilon = a N^{b}$$

$$\alpha = 0.6768\ T^{-1.4968} S^{0.2834} L^{0.1788} R^{0.5692}$$

$$b = -2.2616 - 0.3256\ log(S) + 0.033\ log(L) - 0.1274\ log(R) + 1.1036\ log(T)$$

Figure 13. Equation. Regression model for rutting prediction.

WHEEL WANDER IN PAVEMENT DESIGN

The lateral position of the wheel load is one of the most important variables for flexible pavement design. The lateral position is not a deterministic variable for human-driven trucks. This variable is commonly referred to as wheel wander in the pavement design community, as this term implies its inherent randomness. Given its randomness, flexible pavement design guidelines have considered variable implicitly in a probabilistic way rather than as an explicit input. This section summarizes the studies that incorporate wheel wander into flexible pavement design procedures. In order to understand these studies, one must note the mathematical representation of the wheel wander.

Wheel Wander Definition

Wheel wander can be interpreted as the uncertainty of a lateral position of wheel loads on a lane (see Figure 14). Mathematical representation of wheel wander may be built by defining a variable, noted as d_w, as the distance between the edge of the tire and the road. This distance is not a deterministic value for human-driven trucks. Hence, it should be modeled using probabilistic approaches.

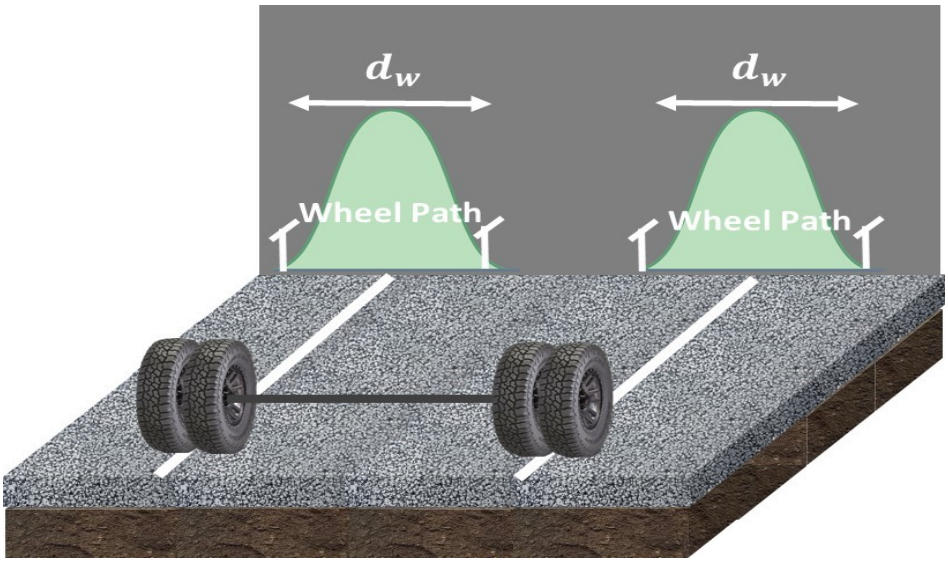

Figure 14. Photo Wheel wander demonstration.

The probabilistic modeling of wheel wander starts with a conventional assumption that a vehicle is inclined to be centered on the lane with uncertainty. For example, its position deviates from its mean location, the center of the lane, with some probability. Traditionally, this assumption is modelled using a zero-mean normal distribution with a known standard deviation (see Figure 15). The value used for standard deviation dictates the wheel wander's level of randomness. The National Cooperative Highway Research Program (NCHRP) (2004) recommends 10 in for the standard deviation.

$$f(d_w) = \frac{1}{\sqrt{2\pi\sigma^2}} e^{-\frac{(d_w-\mu)^2}{2\sigma^2}} \quad where\ \mu = and\ \sigma = standard\ deviation$$

Figure 15. Equation Normal distribution equation.

Current Consideration of Wheel Wander in Pavement Design Procedures

It is important to incorporate the impact of wheel wander while designing a pavement. There are two studies in the literature that developed analytical approaches to consider the wheel wander in pavement design based on the aforementioned definition.

The first approach was developed by NCHRP (2004). It is illustrated in Figure 16, where row B shows the damage accumulation profile, which indicates the maximum used to compute the pavement service life if no wander occurred. In this approach, the average of the predicted damage is computed at five discrete locations. The average is then used as the final damage (see Figure 17). The discrete points are selected by moving −1.28σ from the center five times (see Figure 14). Each jump is assumed to represent 20% of the traffic. It is important to note that this approach could only be used for fatigue cracking prediction. In NCHRP's (2004, 26) study, it states that "for rutting, the guide software modifies the actual pavement responses for the effects of wander and uses this modified response for the calculation of the incremental permanent deformation within each layer." Yet, there is no explanation provided on the response modification.

The second approach, developed by Siddharthan et al. (2017), modifies the pavement structural responses computed by the 3-D Move software to account for the wheel wander. This modification is based on the Monte Carlo simulation. Later, the modified responses are injected to the empirical functions, also used by NCHRP (2004), to predict the damage within in the pavement structure. The steps of the developed approach are listed as follows:

- Draw a sample from the distribution provided in Figure 15's equation.
- Accept the sample if it is not outside of the boundaries (see Figure 14).
- Calculate all critical pavement responses at the accepted sample.
- Repeat the first three steps 10,000 times.
- Generate the cumulative distribution function for each critical pavement response.
- Discretize the cumulative distribution on specific probabilities (e.g., 0, 20, 40, 60, 80, and 100%).

- Extract the responses at the selected probabilities and average them.
- Use averaged responses in the empirical equations and compute the damage.

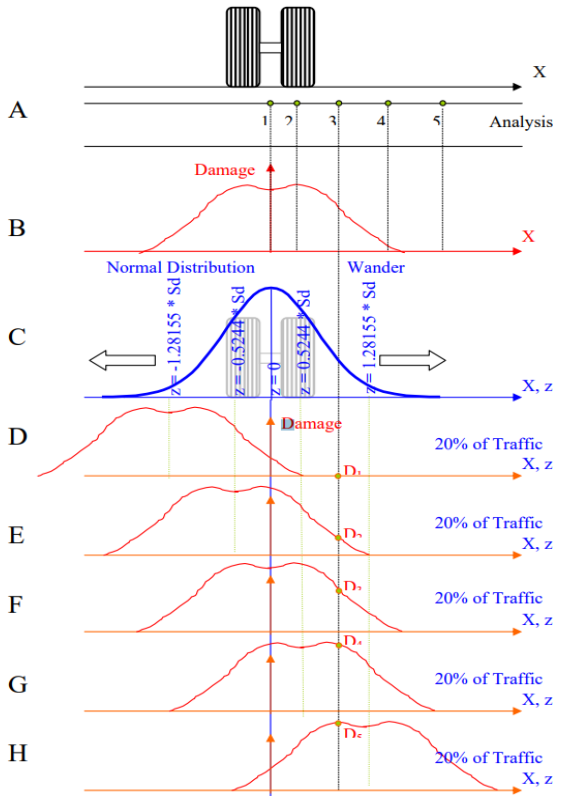

Figure 16. Graph. NCHRP's analytical approach for wheel wander consideration.

Source: NCHRP, 2004

$$D = 0.2D_1 + 0.2D_2 + 0.2D_3 + 0.2D_4 + 0.2D_5$$

Figure 17. Equation. The average of predicted damages.

Wheel Wander Measurement Methods

The aforementioned probabilistic approaches that simulate the impact of wheel wander in pavement design and analysis are based on the assumption that wheel wander follows a zero-mean normal distribution with a known standard deviation (Figure 15). To validate this assumption and have a better understanding of the wheel wander distribution, many studies have been conducted to measure the lateral position of vehicles in the field. Based on measurement methods, these studies are grouped into three categories, including manual survey, video processing, and road instrumentation (Lou and Wang 2013).

Manual Survey

In this method, a reference line was placed on a lane, and an observer recorded the distance between the right rear wheels of the vehicles and the reference line. This method was used when

camera or sensor technology does not exist (Pauls 1925; Taragin 1958). Although this method gave pavement researchers ideas about wheel wander distribution, it was later abandoned due to accuracy and subjectivity concerns.

Video Processing

This method involves processing collected videos to extract the lateral positions of vehicles. Studies utilizing video processing for wheel wander measurement can be classified into two groups, depending on the camera mounting location.

In the first group, a camera is mounted onto a vehicle that tailed the other vehicles in the traffic. The camera records the vehicles' lateral movements as they travel. Shankar and Lee (1985) placed a camera on a van that followed 50 trucks and collected 6 hours of video. The percentage of the truck type recorded in the database represented the actual truck traffic. The distance between the right edge of the truck tire and the left side of the pavement were extracted from the videos by placing a grid on a computer screen. The grid sizes were scaled based on the lane width. Triggs (1997) followed a similar methodology to better understand the effect of approaching vehicles on the lateral position of cars traveling on a two-lane, rural road. All 170 randomly selected cars were recorded by a camera mounted on the research car for an average of 75 min. Lennie and Bunker (2003) measured the lateral position of three multi-combination vehicles (MCVs) to "understand how lane width requirements are influenced by the sideways movement of the trailers and the lateral position of the prime mover." The MCVs were monitored in an urban arterial and highway to study the effect of the surrounding vehicles' drivers' behavioral characteristics. The purpose of the study was to determine if the lanes were wide enough to accommodate MCVs by considering their lateral movements, which were extracted from the videos (see Figure 18).

Figure 18. Photo. A snapshot from video recordings.

Source: Lennie and Bunker 2003

The second group mounted a camera to infrastructure, such as a bridge or a roadway's shoulder, to record the lateral position of the vehicles. Stempihar et al. (2005) placed a camera on the roadway's shoulder for monitoring. Additionally, reference lines were marked on the road in the direction of traffic at set intervals, which helped compute the distance between the edge of the tire and the lane marking (see Figure 19).

A. Reference lines

B. Tire on the reference line

Figure 19. Photo. Data collection system.

Source: Stempihar et al. 2005

Lennie and Bunker's 2005 study also evaluated the impact of MCVs on car drivers' behavioral characteristics, but the methodology was different at this time. Instead of using a car-mounted camera, Lennie and Bunker used an overpass to position the camera. The lateral position of the vehicles was measured by overlaying a transparent sheet with a horizontal scale on the computer screen. Four hours of footage was collected; however, the data size was later reduced because of the high manual processing time. Luo and Wang (2013) followed a similar methodology, where the camera was mounted on an overpass to measure the lateral position of vehicles at five different interstate locations under different conditions, including low and heavy traffic volumes during the day and nighttime as well as in sunny, rainy, and windy weather conditions (see Figure 20). In this study, a reference line was placed on the road to extract the truck's lateral position from the videos

as opposed to overlaying a scaled paper on a computer screen. The purpose of the study was to develop a new wheel-path definition based on the collected data.

Figure 20. Photo. Data collection system developed.

Source: Luo and Wang 2013

Road Instrumentation

In this approach, the lateral position of the vehicles is determined by sensors instrumented on a road surface. Studies using this approach can be grouped into two categories: (i) placing the instrumented mat on road surfaces or (ii) embedding the sensors in road surfaces.

Buiter et al. (1989) placed 120 switch elements side by side with 0.8-in intervals on a mat. Later, this mat was attached to a road surface using double-sided adhesive tape. The switch elements were sensitive to pressure. Thus, they were activated when a wheel passed over them. The lateral position of a wheel, along with the tire footprint, could be extracted by registering which sensors were activated along the mat after each pass. Additionally, this system identified tire types as single, double, or wide-based tires. Blab and Litzka (1995) developed a similar system called the Lateral Displacement System (LDS). Given its high flexibility, LDS can adapt itself to any kind of deformed surfaces. Its switches are 0.6-in-wide and its spacing is at 1.2 in. Two additional tape switches were attached to the LDS to measure vehicle velocities. The system was installed on 27 different road segments to collect data on varying traffic conditions. This study performed regression analysis on the collected data to investigate the relations between the vehicles' wheel wander, lane width, speed, and rutting.

Timm and Priest (2005) embedded three axle-sensing strips in road segments at the National Center for Asphalt Technology Test Track (see Figure 23-A). The stripes were placed with a specific layout, two vertical and one diagonal (see Figure 23-B). Each strip had a cross section of 1 in^2. The length of each vertically placed stripe was 7.2 ft, and the diagonal strip was 10 ft long. The time steps recorded from the strips were injected into the equation shown in Figure 21. Afterwards, the lateral distance of a wheel (y') could be computed using the trigonometric relation given in the equation shown in Figure 22. The data collection system was calibrated using field measurements obtained from using a line of fine sand.

$$x' = \frac{x}{t_3 - t_1}(t_3 - t_1) - f$$

Figure 21. Equation to identify the distance between strips.

Here t_i is the time in which the stamps were recorded by the i^{th} strip. *x* represents the distance between the first and third strips while *f* is the distance between the first and second strips.

$$y' = x' tan\alpha$$

Figure 22. Equation to compute lateral distance.

Here alpha is the angle of the diagonal strip (see Figure 23).

A. Instrumentation

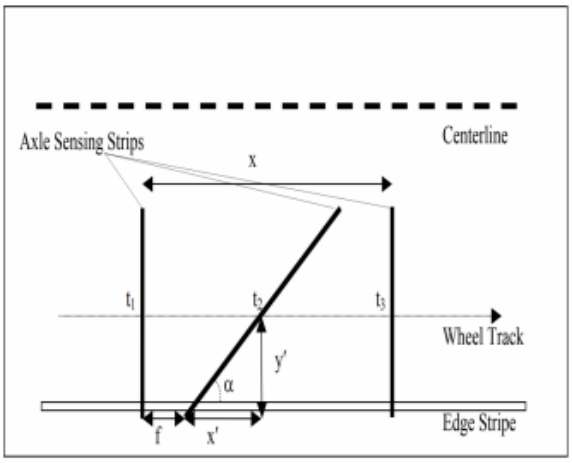

B. Sensor Layout

Figure 23. Photo. Instrumentation (a) and sensor layout (b).

Quantification of Wheel Wander through Pavement Testing

This section summarizes the studies that assess wheel wander's impact on pavement structure using pavement testing.

Al-Qadi et al. (2004) placed more than 500 sensors into 12 pavement sections with varying layer properties, such as thickness and material properties, at the Virginia Smart Road. The length of each section was approximately 330 ft. The purpose of the project was to monitor pavement responses in order to better understand pavement behavior under loading. One such factor studied was the wheel wander, and its impact was assessed by developing a shift factor (Al-Qadi and Nassar 2003). The shift factor was developed by distributing the load over a 3.3-ft-wide strip around the wheel path to obtain the pavement response distribution with respect to the central point. A similar methodology was also followed by Timm et al.'s (2005) study, where researchers developed regression equations that input the lateral position of a wheel and output a pavement response, such as the strain at the bottom of HMA. Shafiee et al.'s 2014 study attempted to quantify the impact of wheel wander on pavement responses. In 2012, approximately 20 sensors, including strain gauges and pressure cells, were installed in two pavement sections at the University of Alberta's Integrated Road Research Facility. Pre-loaded single- and multi-unit trucks were used to measure pavement responses at different offsets, changing between −24 and 24 in. Later, the responses were linked to the Mechanistic-Empirical Pavement Design Guide to perform a sensitivity analysis based on predicted damage.

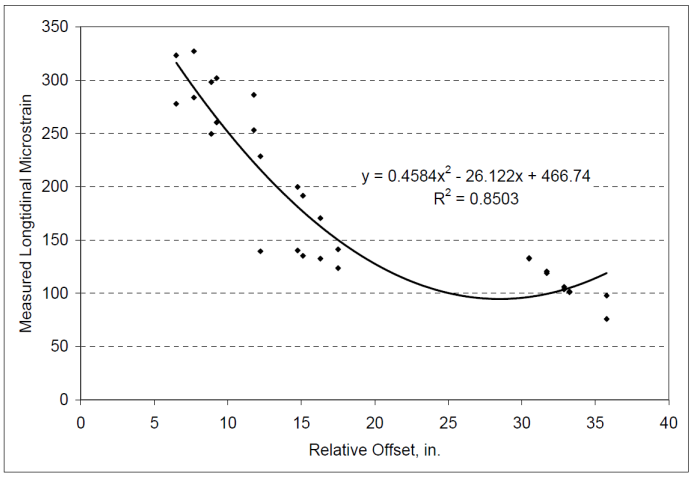

Figure 24. Graph. Offset-Strain regression equation.

Source: Timm et al. 2005

Between 1996 and 1999, the field performance of flexible pavement was monitored at WesTrack (Epps and Jon 2002). Traffic loading was simulated using four trucks composed of a triple-trailer pulled by tandem-axle, class-8 tractors. The trucks were operated autonomously, embedding guidewire on pavement and installing antennas on the front and rear of trucks. These antennas continuously communicated with the guidewires to detect the lateral position of the trucks. By arranging the position of the antennas, the wheel wander could be simulated. The pavement performance was evaluated based on measured rutting, fatigue cracking, and the international

roughness index (IRI). In the case of no wander, a square rutting pattern was observed. The findings highlighted the significance of the wheel wandering effect on long-term pavement performance.

Wu and Harvey (2008) used the heavy vehicle simulator at the University of California's Pavement Research Center to understand how wheel wander affects rutting development within the pavement structure. In order to accomplish this goal, researchers built two identical pavement sections that have 4 in of HMA and 12 in of base. While one of the sections was exposed to channelized load application (i.e., without wander), the wheel wander was simulated on the other one so that the results could be compared to quantify its impact. The wheel wander was simulated in a sweeping pattern, moving the path by 2 in after each load application. The width of the section and the wheel (dual tire assembly) were 40 in and 24 in, respectively. The position of the wheel load in a full cycle was 0, 2, 4, ... 14, 16, 14, 12, ..., 2, and 0 in. Figure 25 shows a measured rutting profile after 3,000 repetitions. Two important observations can be made from this figure: (1) the wheel wander decreased the maximum rutting by approximately 25% and (ii) the location of maximum rutting changed. For the case without wander, the maximum rutting was observed right under one of the tires. As for the case with the wheel wander, it shifted towards the center of the tires. Thus, the wheel wander not only decreased the magnitude, but it also changed the shape of the rutting profile. The study also developed an analytic model for rutting simulation and calibrated it with field measurements.

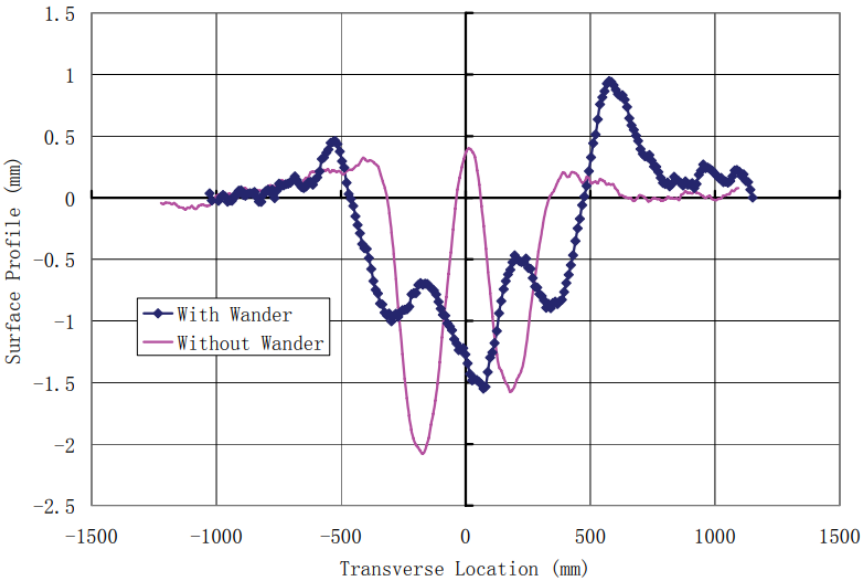

Figure 25. Graph. Rutting profile after 3,000 load repetitions (1mm = 0.04 in).

Source: Wu and Harvey 2008

LATERAL POSITIONING OF CONNECTED AND AUTONOMOUS TRUCKS

Noorvand et al. (2017) researched the influence of truck loading positioning on the long-term performance of flexible pavements. In that study, a scenario-based approach was followed with varying autonomous truck penetrations and lane distributions, including normal, uniform, and

channelized (i.e., no lateral movement) distributions. The impact of these distributions on pavement performance was computed based on developed equivalency factors (EFs), which convert the damage induced by normally distributed truck loadings to other distributions. The AASHTOWare Pavement M-E Design Software was used to run the modified AADTTs, after applying EFs, to simulate the damage accumulation over the pavement service life. Results showed that uncontrolled autonomous trucks, ones with no lateral movement, can significantly increase the damage accumulation rate within pavement. This, however, can be remedied by controlling the wander (e.g., uniform distribution case). The authors noted that the effect of uniform load distribution becomes prevalent with a 50% autonomous truck penetration rate. A similar study was conducted by Chen et al. (2019) that reported similar conclusions.

Zhou et al. (2019) measured the wheel wandering of an autonomous vehicle developed by Texas A&M University. The results showed that lateral position of the autonomous vehicle also follows a normal distribution; however, the standard deviation is much smaller compared to that of human-driven vehicles. Assuming that an autonomous truck would also have the same lateral position distribution as the autonomous vehicle, this study conducted damage analysis using Texas mechanistic-empirical pavement design guidelines. The results showed that narrower wheel wandering caused by autonomous trucks reduced the fatigue life by 20% while it increased the total rutting by 30%. This study also stated that the risk of hydroplaning significantly increased because of high rutting accumulation due to channelized traffic. Uniform distribution of loading was reported as a remedy to mitigate accelerated damage accumulation within the pavement due to autonomous trucks.

The following chapter identifies the platoonable sections based on traffic-density analysis in Illinois.

CHAPTER 3: ILLINOIS PLATOONABLE SECTIONS

METHODOLOGY

A platoonable section is defined as a section in which trucks must be able to travel in a platoon. To assess roadway platoonability, this study used the Illinois Department of Transportation's (IDOT) geographical information systems database (GIST2). GIST2 includes 577,000 road elements with 148,361 mi of Illinois roadways, including various traffic volumes. For trucks, 2,295 mi of Illinois roadways are classified as truck route class 1, which is approved for truck widths of 8.5 ft or less. In addition, 9,703 mi are classified as class 2, which is approved for truck widths of 8.5 ft or less and wheelbases no greater than 65 ft.

A platoonable road segment must meet a certain geometry, speed limit, and traffic volume. The geometry of the road must support traveling at a high speed for an extended distance. In addition, the road should allow sufficient speed for efficient platooning and limit traffic to an acceptable volume level. To minimize platooning interruption, exit ramp density to traffic density should be low.

Geometric Conditions of a Platoonable Roadway

Not all designated truck routes are suitable for platooning; at least two lanes per direction are needed to minimize traffic disruption. Assessing the geometric conditions of a roadway depends on many factors, including surface and truck types as well as road grade and curvature. Some of this information may not be extracted from the GIST2 database. Functional class (FC), however, implicitly considers the geometry of a roadway. For example, interstates and arterials are built to sustain high speeds for extended distances. Thus, the roadway database may be filtered using the roadway FC, which is available in the GIST2 database. Table 1 summarizes the roadway classification system.

Table 1. Functional Classification System for Illinois

Code	Functional Classification
1	Interstate
2	Freeway and Expressway
3	Other Principle Arterial
4	Minor Arterial
5	Major Collector
6	Minor Collector
7	Local Road or Street

FCs 1 through 3 are also listed as a part of the primary arterial system. In this study, FCs 1 and 2 are considered as candidates for platooning. FC 3 is excluded because the roadway type may not always have designated lanes/routes for exits. When a vehicle exits an FC 3 roadway, it must slow down on the outside lane before departure. This presents a challenge for platoons traveling in the outside lane. The efficiency and safety of the platoon is compromised when vehicles slow down. In addition, most FC 3 roadways do not have sufficient truck traffic to justify a platoon formation.

Filtering the data reduces the 577,000 road elements to 15,000. The filtered database has 3,522 mi of roadway; 2,351 mi of the roadway are classified as mainline, which means they contain two or more lanes. Platoonability was analyzed within these 2,351 mi mainline roadway (Figure 25). The remaining miles, such as ramps, collectors, and distributors, were used to determine the location and density of exit ramps and access points.

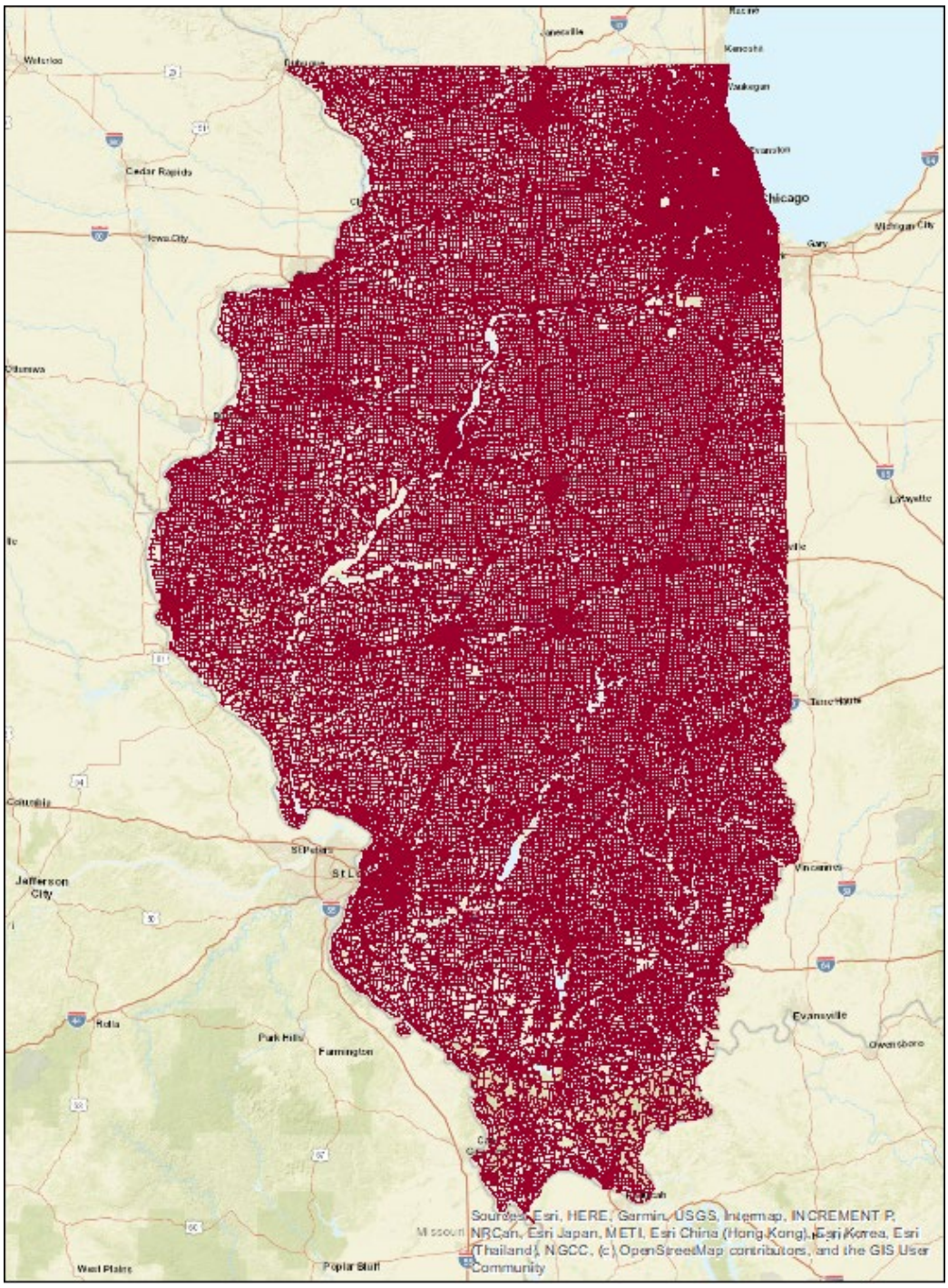

A. Entire GIST2 database

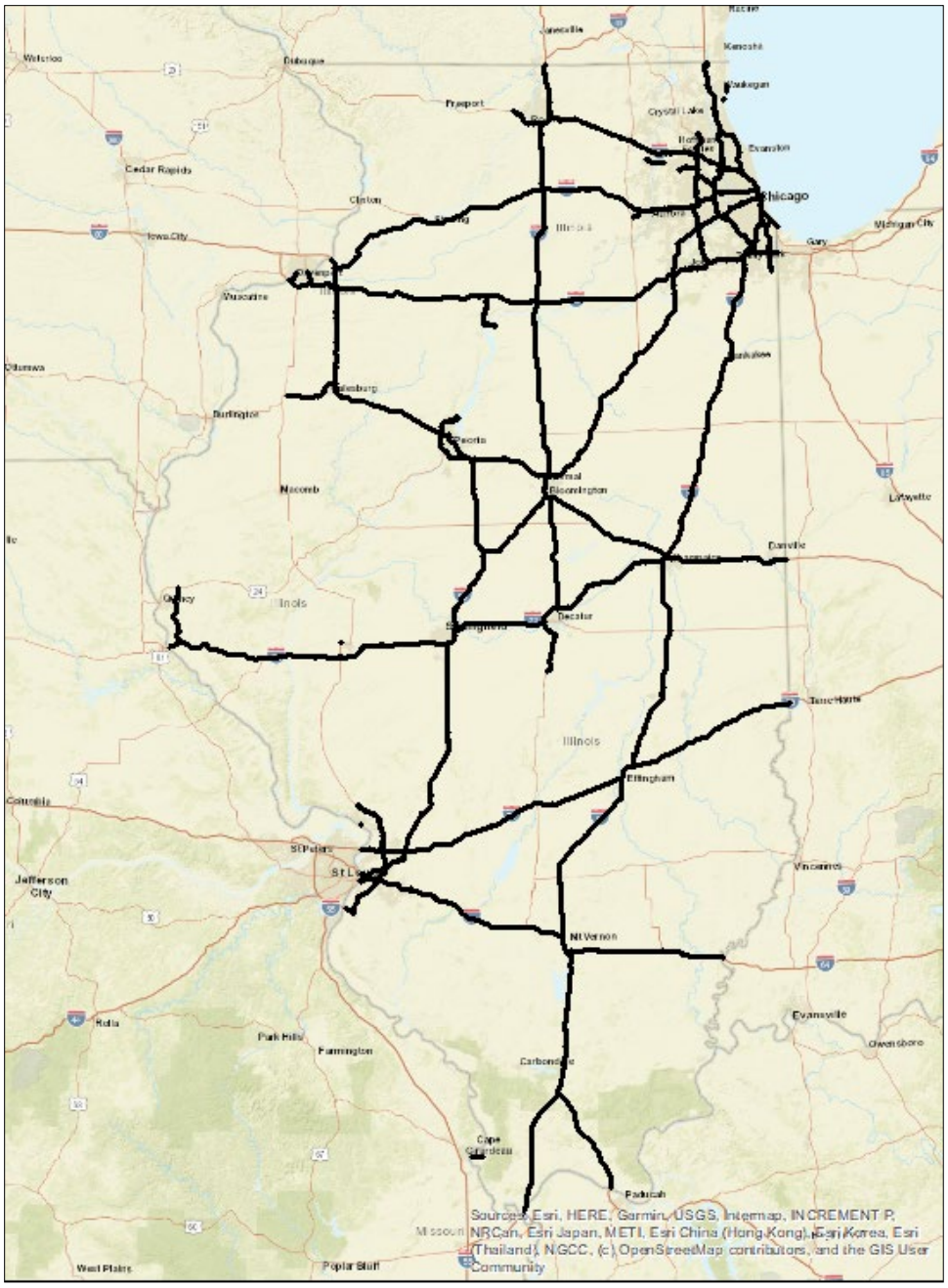

B. FC 1 or FC 2

Figure 26. Entire GIST2 database (A) and FC 1 or FC 2 (B).

Speed Limit

Within the filtered dataset, 57% of the mainline has a speed limit of 70 mph, while 96% has a speed limit of 55 mph or greater. Only 2.7% of the mainline has a speed limit lower than 50 mph. The lowest observed speed limit is 40 mph (Figure 27). Given that truck platooning is most efficient at speeds higher than 55 mph, the dataset was filtered with a speed limit greater than 55 mph (Lammert et al. 2014).

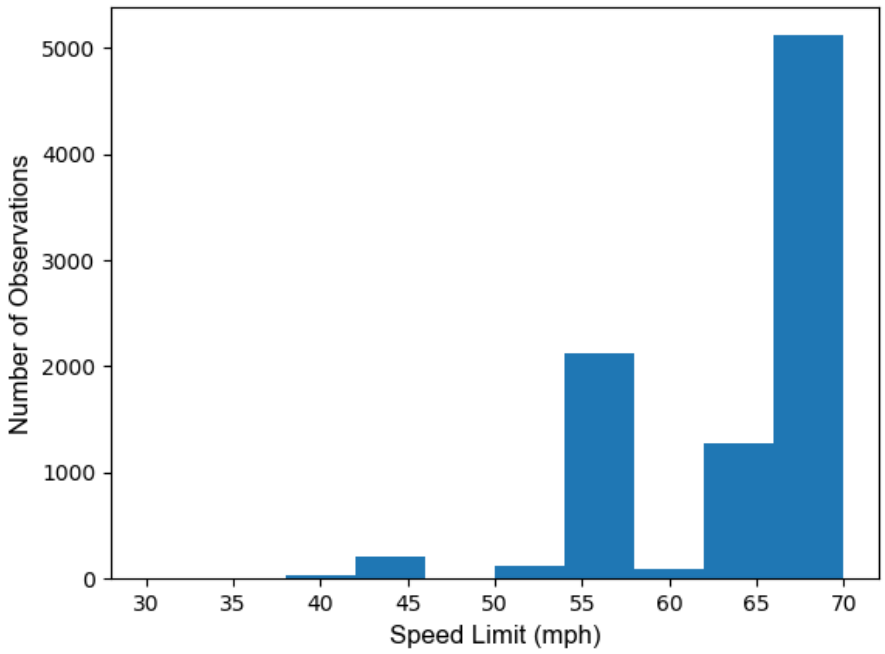

Figure 27. Graph. Speed-limit distribution of the database.

Traffic-density Analysis

Efficiency of platooning is greatly affected by the platoon's ability to freely control its speed. If the platoon could not follow the free-flow speed (FFS) and is forced to follow the traffic-flow speed, any minor disturbance to traffic flow may jeopardize the constant speed needed for efficient platooning.

The level of service (LOS) is the operational conditions within a traffic stream of a highway section. It is a useful indicator of traffic's ability to follow FFSs. A roadway is given one of six measures (A to F) based on its LOS condition (TRB 2000). These measures are described as follows:

- LOS A = A free-flow operation, where vehicle density is very low.
- LOS B = A reasonably free-flow operation, where intervehicle distances are still large.
- LOS C = A near free-flow operation, where vehicles have restricted ability to maneuver, but they are still able to control their speeds.
- LOS D = A critical operation, where speeds start to decline with increasing flows and any minor incident, such as vehicle braking, forms queues.
- LOS E = An operation near or at capacity, where no usable gaps exist in the traffic stream and operation is extremely volatile.
- LOS F = A breakdown in flow, where the demand exceeds the capacity of the roadway.

Based on the aforementioned description, LOS A through C are desired for platoons because vehicles have control over their speeds. LOS D to F vehicle interactions and lane changes are expected to be

relatively high (Wang et al. 2019). For example, merging distances for separated trucks were found to be significantly greater at higher levels of traffic (Liang et al. 2016). Hence, incentives exist to platoon under low-traffic conditions. In this study, LOS C is considered an initial threshold for platooning while LOS D through F may be platoonable under specific traffic conditions.

To determine the LOS of a roadway, the Highway Capacity Manual (TRB 2000) specifies the maximum volume/capacity (v/c) ratios for the roadways at various FFSs. Table 2 presents the v/c ratios for an FFS at 65 mph.

Table 2. Maximum v/c Ratios for FFS at 65 mph

Maximum v/c	LOS
0.3	A
0.5	B
0.71	C
0.89	D
1	E

The volume of a roadway is determined by the number of vehicles expected to pass within a given hour. The capacity of a roadway is a function of the lane width, truck percentage, and FFS. For freeways and highways, which are the road types in the filtered dataset, the capacity calculations were performed using the method reported in the NCHRP's 825 report (Margiotta et al. 2017). The capacity, Cap, is as follows:

$$Cap = \frac{2200 + 10 * (\min(FFS, SL) - 50)}{1 + \%HV/100} * Lanes$$

Figure 28. Equation. Capacity calculation.

where SL is the speed limit (mph) while FFS is the free-flow speed (mph). $Lanes$ represents the number of lanes and $\%HV$ is the percent of heavy vehicles for GIST2, which is the sum of single and multi-unit trucks.

$$FFS = 75.4 - f_{LW}$$

Figure 29. Equation. Free-flow speed as a function of the lane-adjustment factor.

where f_{LW} is the lane-adjustment factor.

$$f_{LW} = \begin{matrix} 6.6 \; if \; LW < 11 \; ft \\ 1.9 \; if \; 11 \; ft \leq LW \leq 12 \; ft \\ 0 \; otherwise \end{matrix}$$

Figure 30. Equation. The lane-adjustment factor as a function of lane width.

where LW represents the lane width (ft).

The capacity calculation is a function of FFS, speed limit, and heavy vehicle traffic. Under specific conditions, platoons may increase traffic capacity from 2% to 25% in the platooning lane (Tsugawa et al. 2016; Wang et al. 2019). The platoon-blocking ramps, however, may decrease traffic capacity and/or stability under certain traffic densities (Calvert et al. 2019). To be conservative, this study did not adjust the traffic capacity with platoons.

IDOT travel statistics can be used to determine the peak hourly, average hourly, and off-peak hourly volumes. As for the volume of the roadways, GIST2 provides the annual average daily traffic (AADT). IDOT provides the hourly percentage of AADT for urban and rural interstates and highways (IDOT 2017). From the traffic patterns, the hourly volumes for peak, average, and off-peak traffic can be summarized as follows:

- 7% of AADT passes through a section during peak hours.
- 4.2% (1/24) of AADT passes through a section on average.
- 2% of AADT passes through a section during off-peak hours.

The average traffic is determined by dividing 100% of AADT by 24 hours. (Each hour in the day carries approximately 4.2% of the AADT.) During peak hours, traffic may go up to 7%, and during off-peak hours, it may go down to 2% because traffic is not uniformly distributed during the day. Using the volume and capacity information, the v/c ratios of the GIST2 database may be determined. Figure 31 maps the results of the analysis for Illinois roadways. During peak hours, the highest v/c ratios are near the Chicago area. During off-peak hours, all roadways are LOS B or better. Figure 32 shows the distribution of the v/c ratios for peak-hour, average, and off-peak-hour traffic cases. Even during peak hours, 94% of all roadways are below a v/c ratio of 0.7 (LOS C), and 87% of the roadways are below 0.5 (LOS B).

Ramp-density Analysis

Vehicle maneuvers near highway exit and entry ramps impact truck platoons. Although studies on special cases exist, the magnitude of the impact, in terms of fuel consumption or traffic disruption, is unknown. This study assumed that a platoon's performance would be affected proportionally by the number of vehicles that the platoon interacts with near exit and entry ramps. Ramp interaction is affected by three factors, including ramp's traffic, density at a given section, and number of trucks in a platoon and spacing between them. If the expected number of vehicle interactions could be determined for a given ramp and a platoon formation, then the density of ramps can be used as a multiplier to vehicle interactions.

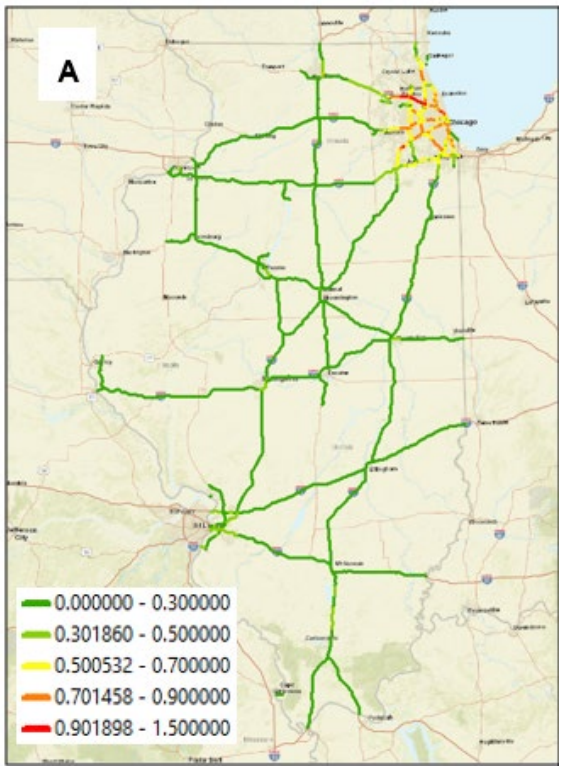

A. The volume-to-capacity ratio at peak hours

B. The volume-to-capacity ratio at off-peak hours

Figure 31. Photo. The volume-to-capacity ratio at peak hours (A) and off-peak hours (B).

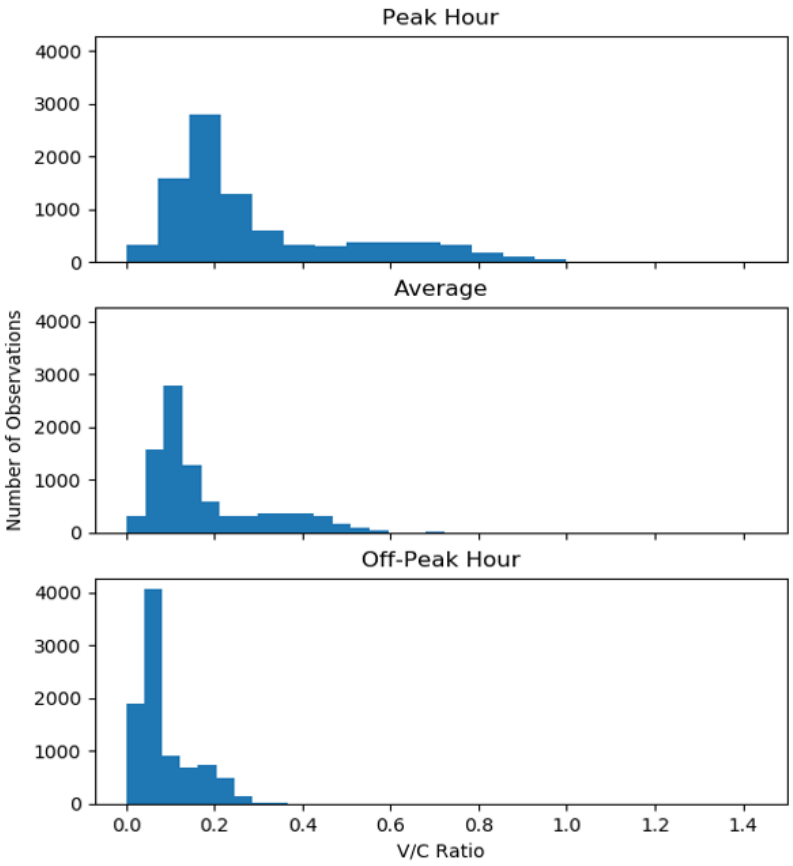

Figure 32. Graph. V/C ratios for various times during the day.

To determine the expected number of interactions for one ramp, the following simplification was made.

$$E(V) = D_t * T_p$$

Figure 33. Equation. Expected number of interactions for one ramp.

where D_t represents traffic density, which is the expected number of vehicles per sec. T_p is time it takes for the platoon to block a ramp in sec.

Parameters D_t and T_p can be further expressed as follows:

$$D_t = AADT * 2 * \frac{Pf}{3600}$$

Figure 34. Equation. Traffic density.

where $AADT$ is annual average daily traffic, and Pf is peak-hour factor as explained in the traffic-density analysis section.

$$T_p = \frac{N_t L_t + (N_t - 1) S_t}{v_P}$$

Figure 35. Equation. Time required by a platoon to block a ramp.

where N_t is the number of trucks in a platoon, L_t is the length of a truck (ft), S_t is the space between trucks (ft), and v_P is the speed of the platoon (ft/sec or 0.68 mph).

For example, consider a platoon of five trucks with a 65-ft spacing and truck length of 60 ft. If the platoon is travelling at 70 mph and passes through a ramp with an AADT of 5,000 vehicles, then the expected number of vehicle interactions are 1.06 ≅ 1 vehicle during the passage of the platoon.

The next step is to determine the ramp density and traffic from the GIST2 database. In the database, the highway exit and entry ramps are marked with the attribute "KY_RT_APP" = 4. They can be filtered and mapped, as given in Figure 36. Out of the 5,573 ramp elements, 8%, or 444, do not have a recorded AADT.

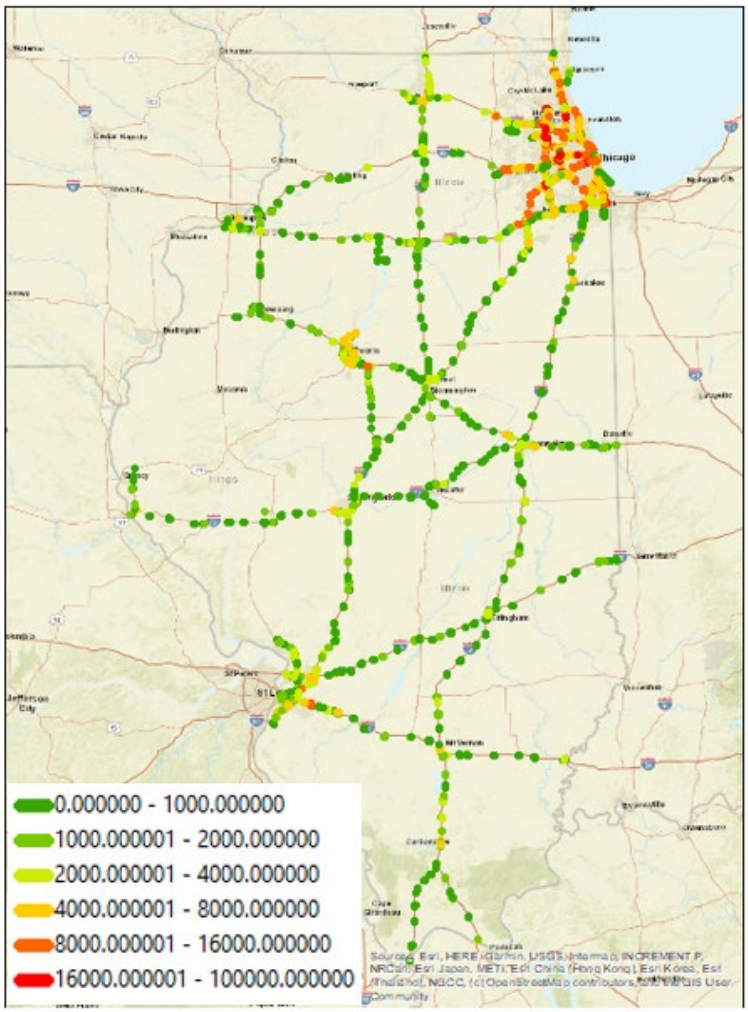

Figure 36. Photo. Location and AADT of ramps.

To mitigate the problem, missing values are replaced with the median ramp AADT—1,687 vehicles. Figure 37 illustrates the distribution of the ramp AADT. Out of all the ramps, 28% have an AADT less than 1,000, 45% have less than 2,000, and 70% have less than 5,000. Only a small amount, 12%, of exit ramps have an AADT higher than 10,000 vehicles—most of which are located around the Chicago area.

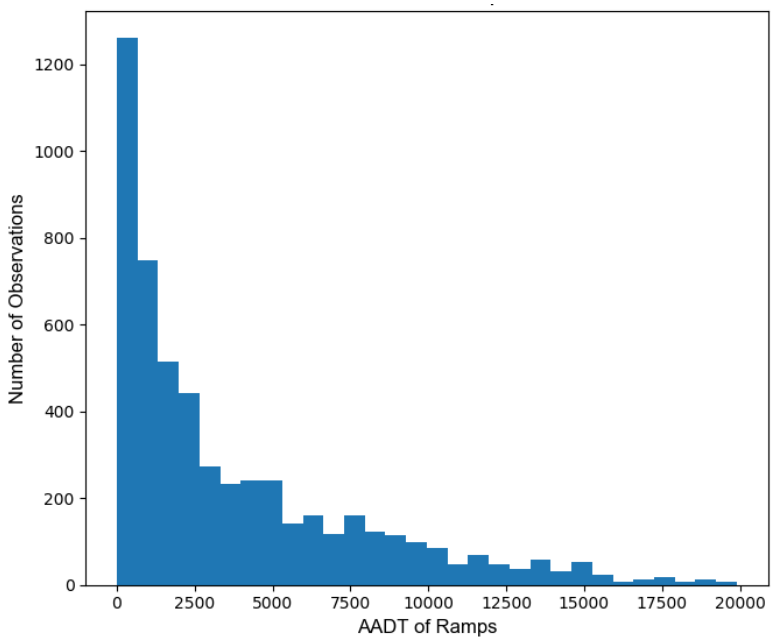

Figure 37. Graph. AADT distribution for ramps.

To determine the expected number of vehicle interactions, the roads were divided into 20-mi-long sections, which approximately amounts to 15 min of travel at 70 mph. Then, the number of ramps were counted and recorded for each 20-mi section. AADT values of each ramp were also summed and averaged by the number of ramps. For example, consider the section in Figure 38. Two ramps exist along the section, with one entry and one exit per ramp per direction. The average AADT of the ramps is 730 vehicles with a standard deviation of 250 vehicles. Thus, this section would be assigned a ramp count of two, per 20 mi, and a ramp AADT of 730 vehicles.

Figure 38. Photo. Example of a 20-mi section near Mineral, Illinois.

Using Figure 33, the expected number of vehicle interactions for a platoon of five trucks and 65-ft spacing during peak hours in this 20-mi segment is 0.15 vehicles per ramp, or 0.3 vehicles in total because there are two ramps. The average distance between two exit ramps in Illinois was found to be 5.21 mi. Figure 39 gives the distribution of the expected number of interactions for each road segment.

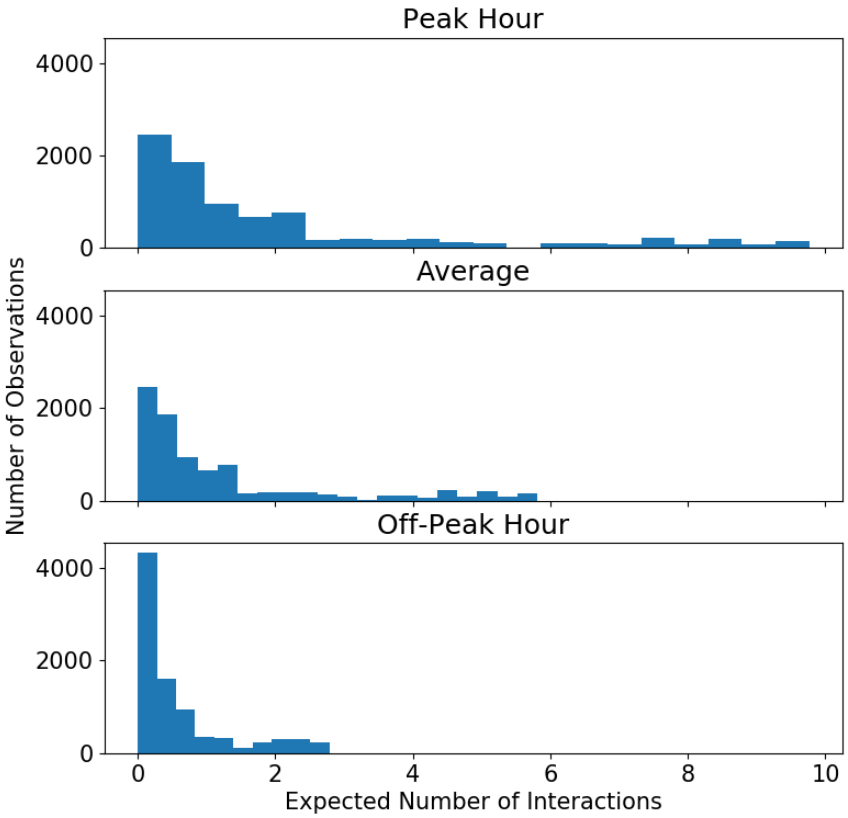

Figure 39. Graph. Expected number of interactions for 20-mi segments for five-truck platoon with 65-ft spacing.

During peak hours, for a five-truck platoon at 65-ft spacing, 45% of all road segments in the database are expected to have less than one interaction, 75% have less than four interactions, and 86 have less than eight. During off-peak hours, all road segments are expected to have less than three interactions.

Analysis of Platoonability

Platoonability is affected by the traffic density and number of interactions near the exit and entry ramps. Both factors were used to determine the platoonability of roadway sections. It is, however, a challenge to accurately define a “platoonable” route. Although there is a relationship between the number of vehicle interactions, traffic density, and platoonability, the exact relationship is case-dependent and affected by human behavior (Liang et al. 2016). In this study, thresholds for platoonability have been determined (see Figure 40).

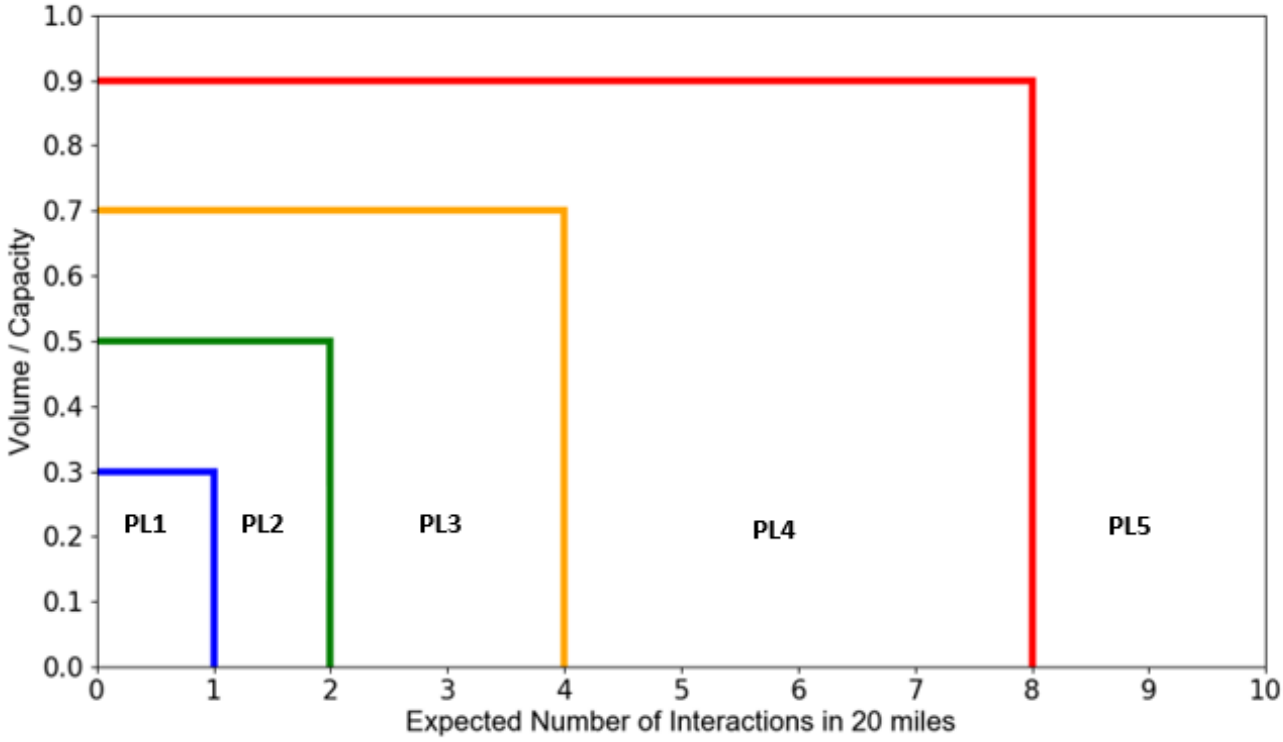

Figure 40. Graph. Platoonability level assignment thresholds.

- Road segments with a v/c $\leq$ 0.3 (LOS A) and an expected number of interactions < one vehicle are labeled Platoonability Level 1 (PL 1).
- Road segments with 0.3 $<$ v/c $\leq$ 0.5 (LOS B) and an expected number of interactions < two vehicles are labeled Platoonability Level 2 (PL 2).
- Road segments with 0.5 $<$ v/c $\leq$ 0.7 (LOS C) and an expected number of interactions less than four vehicles are labeled Platoonability Level 3 (PL 3).
- Road segments with 0.7 $<$ v/c $\leq$ 0.9 (LOS D) and an expected number of interactions less than eight vehicles are labeled Platoonability Level 4 (PL 4).
- Road segments with 0.9 $<$ v/c (LOS E or above) and an expected number of interactions more than eight vehicles are labeled Platoonability Level 5 (PL 5).

These thresholds are selected assuming that the y- and x-axes are independent. From Figure 40, PL 2 sections interact with approximately twice as many vehicles compared to the PL 1 sections. PL 3 sections interact with twice as many vehicles compared to PL 2 sections. PL 4 sections interact with twice as many vehicles compared to PL 3 sections. PL 5 sections are assumed not to be platoonable within the scope of this study because the v/c ratios exceed 0.9 and the stable FFS is unmaintained. Most studies focus on PL 4 sections in terms of capacity increase and traffic disruptions; however, the platoonability of these sections depends on specific conditions and human-behavior assumptions.

This study assumed PL 4 sections as transition zones between platoonable and not platoonable sections.

PL 2 sections are twice as likely to experience breaks from constant speed compared to PL 1 sections. PL 3 sections are twice as likely to experience breaks from constant speed over PL 2 sections, and so on. This is a limitation of the threshold selection because these assumptions are based on empirical capacity and vehicle-interaction calculations. LOS A to B may not correspond to a double in the likelihood of a speed reduction. Similarly, the expected number of interactions may not always reflect the interruption to platooning operation. The exact relationship between these parameters is highly variable and complex.

Platoonability of Illinois roads is determined by three factors: traffic flow at a given hour, ramp density/traffic, and platoon formation. The baseline platoon formation was selected as five trucks at 65-ft spacing. A sensitivity analysis was conducted to determine the impact of this selection. Figure 41 maps the results of the platoonability levels (PL). Even during peak hours, it was found that most PL 3 or below roads were platoonable. Exceptions exist near Champaign, Peoria, and St. Louis. Almost the entire Chicago area is not platoonable during peak hours. During off-peak hours, however, a few segments are PL 4 or above, but the rest of the network is PL 3 or below platoonable. Table 3 provides the percentage of different levels of platoonability.

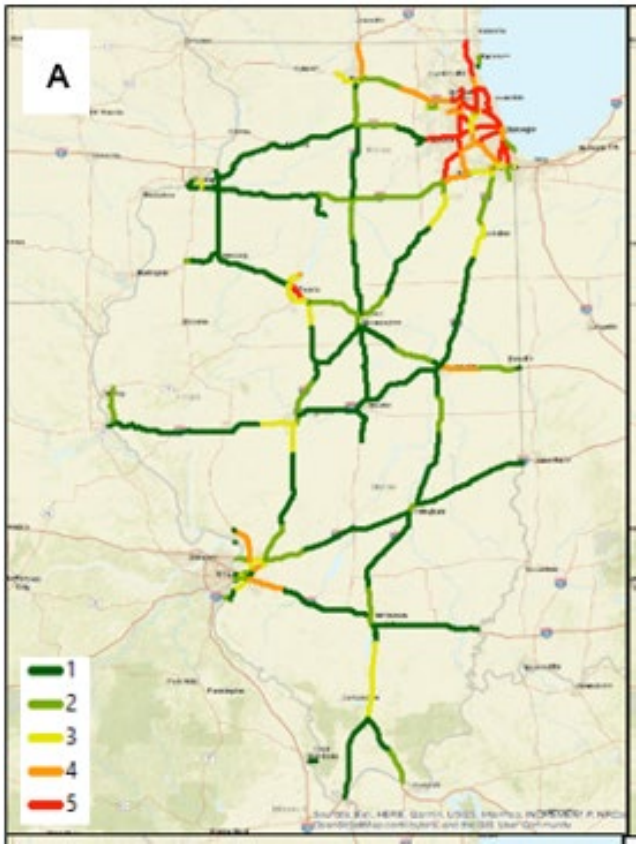

A. Peak hours

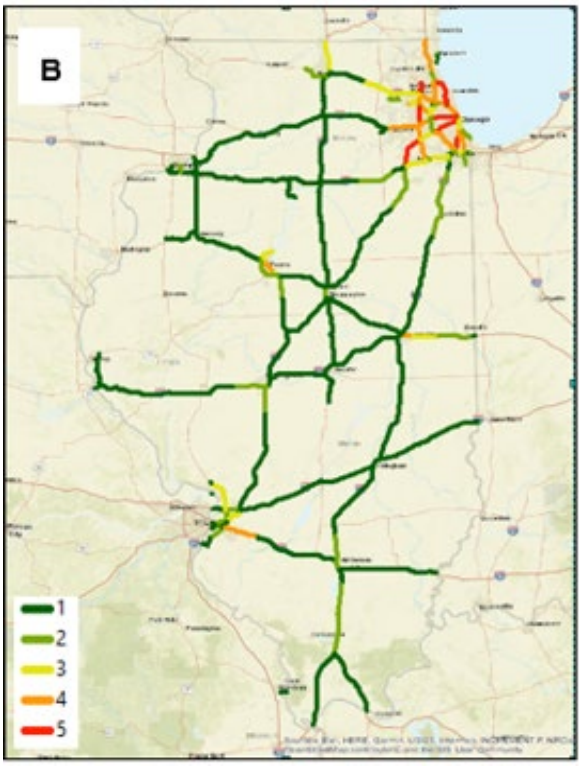

B. Average

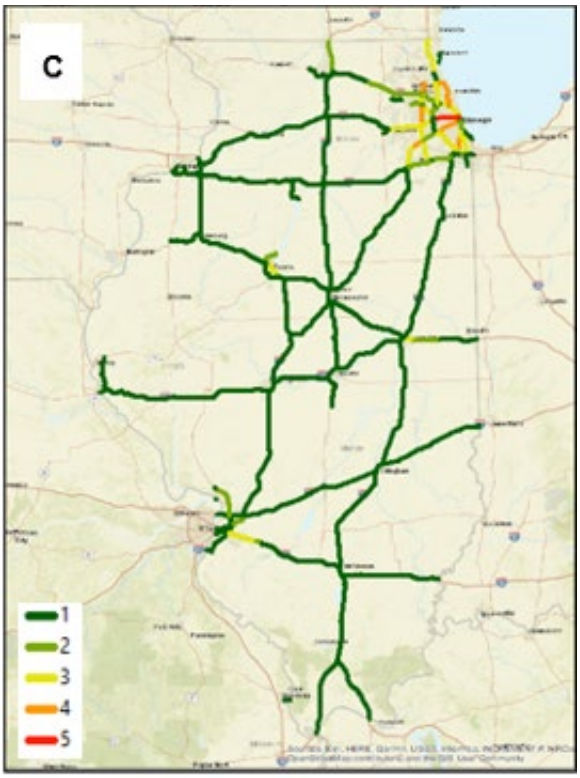

C. Off-peak hours

Figure 41. Graph. PL distribution of Illinois roads during peak (A), average (B), and off-peak (C) hours.

Table 3. PL Percentage of Illinois Roads (FC 1 and FC 2) for Five Trucks with 65-ft Spacing

	PL 1	PL 2	PL 3	PL 4	PL 5
Peak	52%	20%	11%	8%	9%
Average	67%	15%	7%	7%	4%
Off-Peak	81%	8%	7%	3%	1%

During peak-, average-, and off-peak hours, 83%, 89%, and 96% of Illinois roads by length are PL 3 or better, respectively.

Sensitivity to Platoon Formation

The aforementioned results are for a platoon of five trucks with 65-ft spacing travelling at a set speed limit on the road segment. Results may be updated by changing the number of trucks in a platoon and the spacing between them. Table 4 illustrates the results for these analyses during peak hours. Truck platooning is found to be most efficient with truck spacing equal to or less than 65 ft (Lammert and Zhang 2019). With lower spacing, the percentage of platoonable segments is even higher. Moreover, even with a platoon of 10 trucks, nearly 70% of roads are still platoonable. As a baseline, this study uses five trucks at 65-ft spacing as the reference setting.

Table 4. Percentage of Platoonable Segments PL 3 or Better during Peak Hours for Varying Platoon Formations (Baseline Marked with Bold)

	Truck Spacing (ft)							
Number of Trucks	**10**	**15**	**30**	**50**	**65**	**100**	**150**	**200**
2	94%	94%	93%	92%	92%	91%	89%	87%
3	92%	91%	90%	89%	87%	86%	85%	83%
5	87%	86%	86%	85%	**83%**	80%	78%	74%
10	80%	80%	78%	74%	71%	66%	58%	53%
15	74%	72%	67%	65%	62%	54%	46%	39%
20	66%	66%	62%	57%	51%	46%	35%	29%
30	58%	54%	48%	46%	38%	30%	19%	16%

Limitations of Platoonability Analysis

Most platooning studies either focus on low-traffic sections or sections near or at capacity. While the low-traffic sections' platooning performance is easy to predict, it becomes more unpredictable as traffic increases. With a platoon formation of five trucks at 65-ft spacing, 83% of Illinois roadways have a functional class of 1 and 2, and they are platoonable during peak hours. It is, however, difficult to quantify the exact platooning efficiency for various platooning levels. In this study, it was assumed that PL 1 sections are the most platoonable based on road volume and vehicle interactions. PL 2 and PL 3 sections are assumed to be platoonable, although for each increased level number the number of interactions is doubled. This approach may be improved or calibrated as the impact of traffic level on platooning is better quantified.

SUMMARY

Illinois roads were surveyed for platoonability using the Illinois Department of Transportation's GIST2 data. Based on platoonability requirements, functional classes 1 and 2, interstates and freeway/expressways, were selected as initial candidates for platoonability. The total length of the FC 1 and 2 sections is 3,522 mi.

For platoonability determination, volume/capacity ratios of the roadways and the potential conflicts near exit and entry ramps were analyzed. IDOT traffic patterns were analyzed to determine peak and off-peak hour roadway volumes. Potential conflicts were determined by calculating the expected number of vehicle-platoon interactions for a 20-mi section. The v/c ratios and potential conflicts were utilized to assign platoonability levels to roadway sections. Five levels of platoonability were selected based on v/c and potential-conflict thresholds. Pavement sections with platoonability levels 1 through 3 are assumed to be platoonable.

For a benchmark of a five-truck platoon with 65-ft spacing, out of 2,351 mi of FC 1 and 2 roadways, 1,951 (83%) and 2,257 mi (96%) are platoonable during peak and off-peak hours, respectively. A sensitivity analysis was conducted to determine the platoonability of roads when various platoon formations are used. As would be expected, platoons with a higher number of trucks would reduce the percentage of platoonable sections, while reducing the spacing distance would increase platoonable sections.

REFERENCES

Al-Qadi, Imad L., Amara Loulizi, Mostafa Elseifi, and Samer Lahouar. 2004. "The Virginia Smart Road: The Impact of Pavement Instrumentation on Understanding Pavement Performance." *Journal of the Association of Asphalt Paving Technologists* 73 (3): 427–65.

Al-Qadi, Imad L., and Walid N. Nassar. 2003. "Fatigue Shift Factors to Predict HMA Performance." *International Journal of Pavement Engineering* 4 (2): 69-76.

Al-Qadi, Imad L., Egemen Okte, Aravind Ramakrishnan, Qingwen Zhou, and Watheq Sayeh. 2021. *Truck Platooning on Flexible Pavements in Illinois*. Research Report No. FHWA-ICT-21-010. Rantoul, IL: Illinois Center for Transportation. https://doi.org/10.36501/0197-9191/21-010

Beranek, Shannon, and Samuel H. Carpenter. 2009. *Fatigue Failure Testing in Section F*. Research Report ICT-09-058. Rantoul, IL: Illinois Center for Transportation.

Bergenhem, Carl, Steven Shladover, Erik Coelingh, Christoffer Englund, and Sadayuki Tsugawa. 2012. "Overview of Platooning Systems." In *Proceedings of the 19th ITS World Congress,* Oct 22–26, Vienna, Austria, 1–8.

Blab, Ronald, and J. Litzka. 1995. "Measurements of the Lateral Distribution of Heavy Vehicles and Its Effects on the Design of Road Pavements." In *Proceedings of the International Symposium on Heavy Vehicle Weights and Dimensions, Road Transport Technology*, University of Michigan, 389–395.

Bonnet, Christophe, and Hans Fritz. 2000. "Fuel Consumption Reduction in a Platoon: Experimental Results with Two Electronically Coupled Trucks at Close Spacing." *SAE Technical Paper*, No. 2000-01-3056.

Browand, Fred, John McArthur, and Charles Radovich. 2004. "Fuel Saving Achieved in the Field Test of Two Tandem Trucks." https://escholarship.org/content/qt29v570mm/qt29v570mm.pdf

Buiter, R., W. M. H. Cortenraad, A. C. Van Eck, and H. Van Rij. 1989. "Effects of Transverse Distribution of Heavy Vehicles on Thickness Design of Full-Depth Asphalt Pavements." *Transportation Research Record* 1227.

Calvert, Simeon, Wouter J. Schakel, and Bart van Arem. 2019. "Evaluation and Modelling of the Traffic Flow Effects of Truck Platooning." *Transportation Research Part C: Emerging Technologies* 105: 1–22.

Carbaugh, Jason, Datta N. Godbole, and Raja Sengupta. 1998. "Safety and Capacity Analysis of Automated and Manual Highway Systems." *Transportation Research Part C: Emerging Technologies* 6 (1–2): 69–99.

Carpenter, Samuel H., and Shihui Shen. 2006. "Dissipated Energy Approach to Study Hot-Mix Asphalt Healing in Fatigue." *Transportation Research Record* 1970 (1): 178–185.

Castro, María, and José A. Sánchez. 2006. "Fatigue and Healing of Asphalt Mixtures: Discriminate Analysis of Fatigue Curves." *Journal of Transportation Engineering* 132 (2): 168–174.

Chan, Eric. 2016. "SARTRE Automated Platooning Vehicles." *Towards Innovative Freight and Logistics* 2: 137–150.

Chen, Feng, Mingtao Song, Xiaoxiang Ma, and Xingyi Zhu. 2019. “Assess the Impacts of Different Autonomous Trucks’ Lateral Control Modes on Asphalt Pavement Performance.” *Transportation Research Part C: Emerging Technologies* 103: 17–29.

Costello, Bob, and Alan Karickhoff. 2019. “Truck Driver Shortage Analysis.” *The American Trucking Associations: Arlington, Virginia*, 1–17.

Daniel, J. Sias, and Y. R. Kim. 2001. “Laboratory Evaluation of Fatigue Damage and Healing of Asphalt Mixtures.” *Journal of Materials in Civil Engineering* 13 (6): 434–440.

Darabi, Masoud K., Rashid K. Abu Al-Rub, Eyad A. Masad, Chien-Wei Huang, and Dallas N. Little. 2012. “A Modified Viscoplastic Model to Predict the Permanent Deformation of Asphaltic Materials Under Cyclic-Compression Loading at High Temperatures.” *International Journal of Plasticity* 35: 100–134.

Deng, Qichen, and Xiaoliang Ma. 2014. “A Fast Algorithm for Planning Optimal Platoon Speeds on Highway.” *IFAC Proceedings* 47 (3): 8073–8078.

Duret, Aurelien, Meng Wang, and Ludovic Leclercq. 2018. “Truck Platooning Strategy Near Merge: Heuristic-based Solution and Optimality Conditions.” *Presentation in Transportation Research Board 97th Annual Meeting*, Jan. 7–11, Washington, D.C.

Epps, Jon A. 2002. “Recommended Performance-Related Specification for Hot-Mix Asphalt Construction: Results of the WesTrack Project.” *Transportation Research Board Vol. 455*.

Gaudet, Bruce. 2014. “Review of Cooperative Truck Platooning Systems.” *National Research Council Canada* 10, 1–79.

Gungor, O. E., R. She, I. L. Al-Qadi, and Y. Ouyang. 2019. “Optimization of Lateral Position of Autonomous Trucks (OPLAT).” *Presentation Transportation Research Board* No. 19-05626.

Hsu, Tung-Wen, and Kuo-Hung Tseng. 1996. “Effect of Rest Periods on Fatigue Response of Asphalt Concrete Mixtures.” *Journal of Transportation Engineering* 122 (4): 316–322.

Illinois Department of Transportation. 2017. “Illinois State Freight Plan.” *Report,* 1–348.

Illinois Department of Transportation. 2017. “Illinois Traffic Statistics.” *Report,* 1–43.

Kim, Y. R., and D. N. Little. 1989. “Evaluation of Healing in Asphalt Concrete by Means of the Theory of Nonlinear Viscoelasticity.” *Transportation Research Record* 1228: 1–13.

Kim, Y. R., S. L. Whitmoyer, and D. N. Little. 1994. “Healing in Asphalt Concrete Pavements: Is It Real?” *Transportation Research Record* 1454: 1–8.

Lammert, Michael P., Adam Duran, Jeremy Diez, Kevin Burton, and Alex Nicholson. 2014. “Effect of Platooning on Fuel Consumption of Class 8 Vehicles over a Range of Speeds, Following Distances, and Mass.” *SAE International Journal of Commercial Vehicles* 72: 626–639.

Lammert, Michael P., and Chen Zhang. 2019. *Analysis of Platooning Trucks to Better Understand Dynamic Air Flow*. Golden, CO: National Renewable Energy Lab.

Lee, Hyun-Jong, and Y. Richard Kim. 1998. “Viscoelastic Continuum Damage Model of Asphalt Concrete with Healing.” *Journal of Engineering Mechanics* 124 (11): 1224–1232.

Lennie, Sandra C., and Jonathan M. Bunker. 2003. “Evaluation of Lateral Position for Multi-Combination Vehicles.” *Proceedings of the Queensland Main Roads Road System and Engineering Technology Forum*, Bardon, Brisbane, 1–14.

Lennie, Sandra C., and Jonathan M. Bunker. 2005. “Using Lateral Position Information as a Measure of Driver Behaviour around MCVs.” *Road and Transport Research: A Journal of Australian and New Zealand Research and Practice* 14 (3): 62–77.

Liang, Kuo-Yun, Jonas Mårtensson, and Karl H. Johansson. 2016. “Experiments on Platoon Formation of Heavy Trucks in Traffic.” In *IEEE 19th International Conference on Intelligent Transportation Systems*, Rio de Janeiro, Brazil, November 1–4, 1813–1819.

Luo, Wenting, and Kelvin C. P. Wang. 2013. “Wheel Path Wandering Based on Field Data.” PhD diss., University of Arkansas.

Lu, Xiao-Yun, and Steven E. Shladover. 2014. “Automated Truck Platoon Control and Field Test.” *In Road Vehicle Automation*, 247–261.

Mallick, Rajib B., and Tahar El-Korchi. 2013. “Pavement Engineering: Principles and Practice.” *CRC Press*.

Mansourkhaki, Ali, Alireza Sarkar, and Mahmoud Ameri. 2015. “Impact of Different Loading Patterns with Short Duration on the Permanent Strain of Asphalt Mixture.” *Journal of Testing and Evaluation* 43 (4): 853–866.

Margiotta, Richard, and Scott Washburn. 2017. *Simplified Highway Capacity Calculation Method for the Highway Performance Monitoring System*. FHWA Technical Report No. PL-18-003.

McAuliffe, Brian, Mark Croken, Mojtaba Ahmadi-Baloutaki, and Arash Raeesi. 2017. “Fuel-Economy Testing of a Three-Vehicle Truck Platooning System.” https://escholarship.org/content/qt7g37w4fb/qt7g37w4fb.pdf

Motevalizadeh, Seyed Mohsen, Pooyan Ayar, Seyed Hossein Motevalizadeh, Sadegh Yeganeh, and Mahmoud Ameri. 2018. “Investigating the Impact of Different Loading Patterns on the Permanent Deformation Behaviour in Hot Mix Asphalt.” *Construction and Building Materials* 167: 707–715.

Muratori, Matteo, Jacob Holden, Michael Lammert, Adam Duran, Stanley Young, and Jeffrey Gonder. 2017. *Potentials for Platooning in US Highway Freight Transport*. NREL/CP-5400-67618. Golden, CO: National Renewable Energy Lab.

National Cooperative Highway Research Program. 2004. *Guide for Mechanistic-Empirical Design of New and Rehabilitated Pavement Structures*. Final Report NCHRP Project 1-37A.

Nejad, Fereidoon Moghadas, H. Sorkhabi, and Mohammad M. Karimi. 2015. “Experimental Investigation of Rest Time Effect on Permanent Deformation of Asphalt Concrete.” *Journal of Materials in Civil Engineering* 28 (5): 06015016.

Nowakowski, Christopher, Steven E. Shladover, Xiao-Yun Lu, Deborah Thompson, and Aravind Kailas. 2015. “Cooperative Adaptive Cruise Control (CACC) for Truck Platooning: Operational Concept Alternatives.” https://escholarship.org/content/qt7jf9n5wm/qt7jf9n5wm.pdf

Nowakowski, Christopher, Deborah Thompson, Steven E. Shladover, Aravind Kailas, and Xiao-Yun Lu. 2016. “Operational Concepts for Truck Cooperative Adaptive Cruise Control (CACC) Maneuvers.”

In *Transportation Research Board 95th Annual Meeting*, Washington D.C., no. 16-4462, 1–16.

Palvadi, Sundeep, Amit Bhasin, and Dallas N. Little. 2012. "Method to Quantify Healing in Asphalt Composites by Continuum Damage Approach." *Transportation Research Record* 2296 (1): 86–96.

Pauls, J. T. 1925. "Transverse Distributions of Motor Vehicle Traffic on Paved Highways." *Public Roads* 6 (1): 1–13.

Pierce, Dave, and Dan Murray. 2014. "Cost of Congestion to the Trucking Industry." *American Transportation Research Institute*.

Schapery, Richard A. 1984. "Correspondence Principles and a Generalized Integral for Large Deformation and Fracture Analysis of Viscoelastic Media." *International Journal of Fracture* 25 (3): 195–223.

Shafiee, Mohammad Hossein, Somayeh Nassiri, P. Eng, and Alireza Bayat. 2014. "Field Investigation of the Effect of Operational Speed and Lateral Wheel Wander on Flexible Pavement Mechanistic Responses." *Transportation 2014: Past, Present, Future—2014 Conference and Exhibition of the Transportation Association of Canada, Canada,* 1–22.

Shan, Liyan, Yiqiu Tan, Shane Underwood, and Y. Richard Kim. 2010. "Application of Thixotropy to Analyze Fatigue and Healing Characteristics of Asphalt Binder." *Transportation Research Record* 2179 (1): 85–92.

Shankar, P. R., and C. E. Lee. 1985. "Lateral Placement of Truck Wheels within Highway Lanes." *Transportation Research Record* 1043: 33.

Siddharthan, Raj V., Mahdi Nasimifar, Xiaoshu Tan, and Elie Y. Hajj. 2017. "Investigation of Impact of Wheel Wander on Pavement Performance." *Road Materials and Pavement Design* 18 (2): 390–407.

Stempihar, J. J., R. C. Williams, and T. D. Drummer. 2005. "Quantifying the Lateral Displacement of Trucks for Use in Pavement Design." *Presentation Transportation Research Board Preprint*, Washington, DC.

Taragin, Asriel. 1958. "Lateral Placements of Trucks on Two-Lane Highways and Four-Lane Divided Highways." *Journal of Highway Research* 30 (3): 71–75.

Timm, David H., and Angela L. Priest. 2005. *Wheel Wander at the NCAT Test Track*. NCAT Report No. 05-02.

Transportation Research Board. 2000. *"*Highway Capacity Manual*." Transportation Research Board Publications, Washington, DC*, 1-1207.

Triggs, Thomas J. 1997. "The Effect of Approaching Vehicles on the Lateral Position of Cars Travelling on a Two-lane Rural Road." *Australian Psychologist* 32 (3): 159–163.

Tseng, Kuo-Hung, and Robert L. Lytton. 1990. "Fatigue Damage Properties of Asphaltic Concrete Pavements." *Transportation Research Record* 1286: 1–14.

Tsugawa, Sadayuki. 2014. "Results and Issues of an Automated Truck Platoon within the Energy ITS project." *In 2014 IEEE Intelligent Vehicles Symposium Proceedings,* Dearborn, USA, June 8–11, 642–647.

Tsugawa, Sadayuki, Sabina Jeschke, and Steven E. Shladover. 2016. “A Review of Truck Platooning Projects for Energy Savings.” *IEEE Transactions on Intelligent Vehicles* 1 (1): 68–77.

Qi, Xicheng, and Matthew W. Witczak. 1998. “Time-Dependent Permanent Deformation Models for Asphaltic Mixtures.” *Transportation Research Record* 1639 (1): 83–93.

Underwood, B. Shane, and Waleed Abdelaziz Zeiada. 2014. “Characterization of Microdamage Healing in Asphalt Concrete with a Smeared Continuum Damage Approach.” *Transportation Research Record* 2447 (1): 126–135.

U.S. Department of Transportation, Bureau of Transportation Statistics. 2018. *Transportation Statistics Annual Report 2018*. Washington, DC. https://doi.org/10.21949/1502596.

Van Maarseveen, Sander. 2017. “Impacts of Truck Platooning at Motorway On-Ramps: Analysis of Traffic Performance and Safety Effects of Different Platooning Strategies and Platoon Configurations Using Microscopic Simulation.” Master’s diss., TU Delft.

van Nunen, Ellen, Francesco Esposto, Arash Khabbaz Saberi, and Jan-Pieter Paardekooper. 2017. “Evaluation of Safety Indicators for Truck Platooning.” *In 2017 IEEE Intelligent Vehicles Symposium (IV)*, Redondo Beach, USA, June 11–14, 1013–1018.

Wang, Meng, Sander van Maarseveen, Riender Happee, Onno Tool, and Bart van Arem. 2019. “Benefits and Risks of Truck Platooning on Freeway Operations near Entrance Ramp.” *Transportation Research Record* 2673 (8): 588–602.

Wu, Rongzong, and John T. Harvey. 2008. “Evaluation of the Effect of Wander on Rutting Performance in HVS Tests.” In *Proceedings of the 3rd International Conference on Accelerated Pavement Testing,* Madrid, Spain, October 1–3, 1–14.


Illinois Department
of Transportation


ILLINOIS